Eur. Phys. J. Plus (2024) 139:488
https://doi.org/10.1140/epjp/s13360-024-05282-0

THE EUROPEAN PHYSICAL JOURNAL PLUS

Regular Article

Mathematical Modeling of Regime Shifts in Fluctuating Environments: The Impact of Allee Effects and Cooperation

Biswajit Paul[1], **Bapin Mondal**[2,a], **Uttam Ghosh**[2]

[1] Department of Mathematics, Government General Degree College, Chapra, West Bengal Nadia 741123, India
[2] Department of Applied Mathematics, University of Calcutta, Kolkata 700009, India

Received: 29 March 2024 / Accepted: 15 May 2024

Abstract In this paper, we investigate the deterministic and stochastic behaviour of the prey-predator model with cooperation and the mate-finding Allee effect. The stochasticity in the prey-predator model arises due to environmental or genetic fluctuations. The deterministic model is reduced to a stochastic model through the introduction of environmental fluctuations in model parameters. We discussed the dynamical behaviour of deterministic prey-predator models such as positivity, boundedness, different types of equilibrium and their local stability with different bifurcations. By allowing both prey and predator species to be affected by stochastic perturbations, we modify the proposed model to its stochastic counterpart. We investigate the uniqueness of positive global solutions, the existence of stationary distributions, etc., of stochastic model solutions. The simulation results for the stochastic system demonstrate that fluctuations in the ecosystem due to stochastic perturbations are highly sensitive to environmental noise intensities. With the increase in environmental fluctuation, there is a shift in regime i.e., noise-induced transition from the attractor to predator extinction. Stochastic confidence ellipses are used to analyze the effect of noise-induced transitions.

1 Introduction

Interplay among different populations plays an important role in ecology. It deals with the variation of population size and density for one or more species depending on several factors [1, 2]. Several models were developed by the mathematician and ecologist, describing the dynamical behavior of spatial-temporal density of the species [3]. In ecosystem the modeling population dynamics is too challenging due to the existence of a large number of species and different interactions. Prey-predator interaction is one of the most common interactions in ecology, as described by [1]. In ecosystems, interactions between species occur in different ways. To know more about the evolution of ecological systems and the interaction between species, we have to concentrate on the study of population dynamics.

There are a lot of discoveries in mathematical modeling after the work of Lotka [2] and Volterra [4]. In the ecological system, the most significant factor is a functional response, which defines the predator's consumption pattern. Basically the functional response can be separated by two classes one of them is prey dependent [5, 6] and another is both prey and predator dependent [7, 8]. In the classical Lokta-Volterra model [2, 4], the Holling type I functional response (linear) is employed, represented by $f(N) = \lambda N$, where $\lambda(> 0)$ is the proportionality constant, and $N(t)$ is the density of the species population. However, the Holling type I functional response is unbounded, making it unsuitable for all biological models of ecological systems. To address this limitation, Holling introduced another functional response known as Holling type II, defined as $f(N) = \frac{\lambda N}{1+h\lambda N}$, where $h(> 0)$ is the half saturation constant. The Holling type II functional response is bounded and proves to be more applicable in many ecological systems compared to Holling type I, as it avoids unbounded growth. Several researchers [9, 10] used Holling II functional response in their model. We know that the functional response are either prey dependent or predator dependent sometimes both prey and predator dependent. But sometimes due to the fact it can be derived from other criteria. In [11], the author shows that the intermediate predator's density is used in principle predator and the intermediate predator dominates the density of prey population.

Cooperation is a fundamental process where a group of species involved for their mutual benefit and it plays an important role in ecology. The experimental results show that in nature the predators hunt their prey together as a group [12]. Hunting in a group take more advantages like increase the success rate, decrease the distance of chasing [13], the chances of catching more prey increase [14]. The cooperative behaviour observe for some predators for hunting upon their prey and they also create fear. For example, wolves cooperate for hunting their prey and also attack indirectly [15]. In [16], the author has shown that in the presence of hunting cooperation the system exhibits stable coexistence equilibrium, and the model exhibit complex dynamics. They also noticed that hunting cooperation creates a positive relationship between population density and per capita growth rate. In [17], the author discuss

[a] e-mail: bapinmondal1@gmail.com (corresponding author)

Published online: 05 June 2024

about hunting cooperation in discrete predator-prey system and shown that the chaotic regime shift with the help of period doubling bifurcation. Due to increase of hunting cooperation the system goes to stable from chaotic dynamics. There is very little research work about hunting cooperation [18–20]. The author in [20] shown that hunting cooperation generate fear in prey and the system goes to extinction. In similar manner the author in [21] discussed about modified Leslie-Gower model with fear in prey and cooperation in predator and shown that the fear effect is more applicable for stabling the system than hunting cooperation. In [19], the author has shown that the hunting cooperation in a diffusive system positively acts as the coexistence of both populations.

In nature, most of the species experiences cooperative behaviour for feeding, mating condition, environmental restriction and cooperative defense [22] and the density of the population depend on this parameters. Also there is another factor which changes the density of the population and this is known as Allee effect [23]. For a more realistic upgrade, the Allee effect can be implemented to introduce a non-monotonous per capita growth rate for the interacting species. American ecologist professor W.C. Allee [24] first introduced the concept of the Allee effect. The Allee effect measures population decrement in per capita growth rate at low population density i.e., the individual fitness is directly proportional to the density of the population. Allee effect acts inbreeding depression, annulment or defense predator for environmental condition, mate finding problem etc [23, 25]. Allee effects can be categorized into two types: strong and weak. Strong Allee effects are characterized by negative population growth rates at low densities, whereas weak Allee effects exhibit lower but not negative population growth rates at low densities. Several studies have shown that the dynamics of the prey-predator model hugely change due to Allee effect [26–28]. In a prey-predator system, the predator population may experience behaviors similar to the mate-finding Allee effect due to various factors. Firstly, when prey populations decrease, predators may struggle to find enough food for energy, affecting their ability to find mates and reproduce. Secondly, a drop in prey density reduces the chances for predators to come across potential mates, especially in species where choosing a mate is crucial for successful reproduction. Several mechanisms contribute to the Allee effect in predators, including the lack of mating partners, limited sperm supplies, and low fertilization efficiency [29, 30]. These factors collectively shape the mate-finding Allee effect in predator populations, influencing the dynamics of the entire ecosystem.

The stochasticity is a natural fact in ecosystem. It may create extinction for the population although the deterministic nature is persist for a long time [31]. The discussion of different noise induced phenomena in the organism make a great deal in the ecosystem. There are two types of stochasticity namely environmental and demographic stochasticity. Environmental stochasticity corresponds to environmental fluctuation for instant and it changes the growth rate of the population [32] and demographic stochasticity deals with individual inconsistency. In demographic case it has a large impact on small species whereas environmental stochasticity generate extinction for the small and large individuals. There are several research papers [33–35] have been discovered on environmental stochasticity where the effect of coexistence, extinction, harvesting scenario observed due to white noise. In the deterministic setup we see that the model parameters are assume to be constant and in general the parameters are effected by environmental fluctuation. Using the white noise the system changes drastically from its deterministic nature. In [18] the author shown that due to high fluctuation the stochastic system goes to extinction. So it is clear that there are many studies [36–38], where the solution with deterministic forms that don't correlate with environmental fluctuations, which are important components of ecosystems. There are some difficulties in mathematical modeling for the deterministic sense. In general, difficulty arises for perfect data fit and future dynamics of the system correctly [39]. In [6] the author shows that the birth rate, competition coefficient, carrying capacity, and other parameters are affected by environmental fluctuation.

In this paper, we proposed a two-dimensional prey-predator model with environmental fluctuation in the growth rate of prey and death rate of predator population, considering the effects of mate-finding Allee in predator growth and hunting cooperation. Here, we use the SSF technique to draw a confidence ellipse in the interior of a stable equilibrium point. Also using the technique we discuss the regime shift from one stable zone to other.

The nobility of this paper are highlighted below:

- The proposed work introduces a two-dimensional prey-predator model with environmental fluctuations, integrating mate-finding Allee effect into predator growth and hunting cooperation.
- We identify four interior equilibrium points of our system through numerical analysis.
- The SSF technique is employed to draw a confidence ellipse within the interior of a stable equilibrium point.
- We observed a regime shift occurring with the increase in environmental fluctuation.
- We also observed that high environmental fluctuation leads to predator extinction.

This paper is organized as follows: In section 2, we formulate the model. In Section 3, we examine positivity and boundedness of the solution, different types of equilibria and their stability with a geometric approach and prove different types of bifurcations (Saddle-Node, Hopf) for deterministic model. In Section 4, we discuss the numerical simulation for deterministic model. In Section 5, we discuss the stochastic form of the proposed model. Here, we show the uniqueness and existence of global positive solution, stationary distribution, persistence and extinction of the stochastic model solution. In the next section, a stochastic model is numerically simulated. We present some important results in the last section.

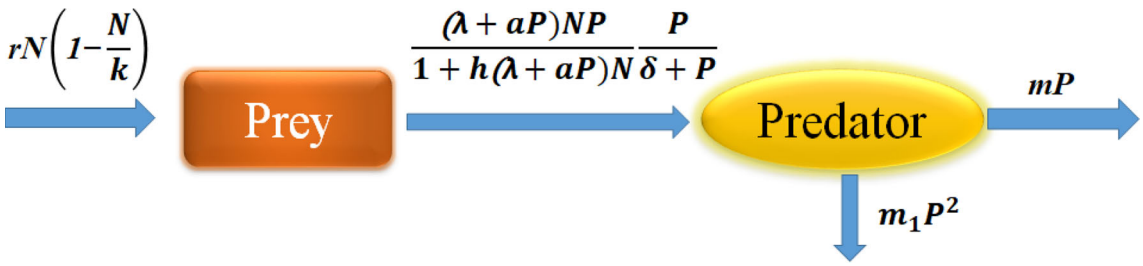

Fig. 1 Schematic diagram of our system

Table 1 Details of parameters with dimension

Parameters	Description	Dimension
r	Growth rate of prey	T^{-1}
k	Carrying capacity	*Biomass*
λ	Attack rate of predator	$Biomass^{-1}T^{-1}$
a	Cooperation coefficient	$Biomass^{-2}T^{-1}$
h	Predator handling time	T
ϵ	Conversion coefficient	1
δ	Allee effect constant	*Biomass*
m	Death rate of predator	T^{-1}
m_1	Death rate of predator due to inter species competition	$Biomass^{-1}T^{-1}$

2 Model formulation

To formulate the model, we consider a one-prey and one predator population. Let $N(t)$ and $P(t)$ be the population density of prey and predator at any time t, respectively with the birth rate of prey being r and carrying capacity k. The model is formulated considering the following assumptions:

(1) This model integrates the inherent environmental capacity to support the prey population, while also considering its reproductive potential. The prey population's growth is influenced by its intrinsic growth rate and the carrying capacity of its habitat.
(2) Predator populations exhibit a cooperative hunting strategy.
(3) Functional response is consider as Holling type II, due to cooperation its functional format is considered as $\frac{(\lambda+aP)NP}{1+h(\lambda+aP)N}$, where the parameters are given in Table 1.
(4) Predator population follows the mate finding Allee effect.
(5) Predator populations engage in intra-specific competition.
(6) Environmental fluctuations impact the birth rate of the prey population and the death rate of the predator population.

Incorporating the first five assumptions, the dynamics of any predator-prey model can be expressed in terms of ordinary differential equations which are as follows:

$$\begin{aligned}\frac{dN}{dt} &= rN\left(1-\frac{N}{k}\right)-\frac{(\lambda+aP)NP}{1+h(\lambda+aP)N}\equiv f(N,P),\\ \frac{dP}{dt} &= \frac{\epsilon(\lambda+aP)NP}{1+h(\lambda+aP)N}\frac{P}{\delta+P}-mP-m_1P^2\equiv g(N,P),\end{aligned} \tag{1}$$

with the initial conditions $N(0)>0,\ \ P(0)\geq 0$ and the details of parameters are shown in Table 1. We have provided a schematic diagram depicting the dynamic interactions between prey and predators in Fig. 1. Based on our knowledge, the first five assumptions for the continuous model have not been considered, and not study the stochasticity has been studied using the SSF technique.

Stochastic predator-prey models offer a broader understanding of ecological community dynamics, especially amid unpredictable environmental fluctuations. Environmental elements like climate variations, earthquakes, and socio-political disruptions such as wars and food shortages significantly influence the birth and mortality rates within ecological systems. These influential factors are often regulated randomly, reflecting the inherent unpredictability of natural systems. By incorporating these factors, researchers can explore the effects of uncertainty and randomness on population dynamics and community interactions, thus improving the precision of predictions and our grasp of ecosystem resilience [32, 40]. Ultimately, integrating environmental noise into predator-prey models represents a crucial step toward enhancing their realism and predictive capacity, aligning more closely with the variability and uncertainties observed in real-world ecological systems [18, 41].

To include the environmental fluctuations in the system replace the intrinsic birth term $rN(t)$ by $rN(t)+\sigma_1 N(t)dB_1(t)$ and the death term $mP(t)$ by $mP(t)+\sigma_2 P(t)dB_2(t)$ in the deterministic model (1) then it reduces to:

$$\begin{aligned} dN(t) &= \left[rN(t)\left(1-\frac{N(t)}{k}\right)-\frac{(\lambda+aP(t))N(t)P(t)}{1+h(\lambda+aP(t))N(t)}\right]dt+\sigma_1 N(t)dB_1(t),\\ dP(t) &= \left[\frac{\epsilon(\lambda+aP(t))N(t)P(t)}{1+h(\lambda+aP(t))N(t)}\frac{P(t)}{\delta+P(t)}-mP(t)-m_1P(t)^2\right]dt+\sigma_2 P(t)dB_2(t), \end{aligned} \tag{2}$$

subject to the same initial condition, where $B_1(t)$ and $B_2(t)$ are independent white noise. Several methods can be used to discuss population dynamics for nonlinear deterministic models, such as the Lyapunov method, Jacobian matrix method, Coincidence degree theory, etc. But some research works are available for the nonlinear stochastic system [42–45] considering the Ito integral formula. In this paper, we consider the application of the Ito integral formula to discuss the long-term behaviour of the population and use stochastic sensitivity analysis to identify the existence of regime shift.

3 Mathematical analysis of deterministic model

In this section, we shall investigate the different complex dynamics of the deterministic model (1). In the next subsections, we shall establish the positivity as well as boundedness of the solution, find different types of equilibria and their local stability, and study different bifurcation analyses for the deterministic model.

3.1 Positivity and boundedness of the solution

Positivity implies that the populations of both prey and predators cannot be negative. In a realistic ecological scenario, it's not possible for the number of prey or predators to be less than zero. Therefore, the populations must always remain positive or non-negative. It is clear that the initial population is always non-negative i.e., $N(0)>0,\ P(0)\geq 0$. Integrating both sides of the system (1) and we get,

$$\begin{aligned} N(t) &= N(0)\exp\left(\int_0^t\left[r\left(1-\frac{N(t)}{k}\right)-\frac{(\lambda+aP(t))P(t)}{1+h(\lambda+aP(t))N(t)}\right]dt\right),\\ P(t) &= P(0)\exp\left(\int_0^t\left[\frac{\epsilon(\lambda+aP(t))N(t)}{1+h(\lambda+aP(t))N(t)}\frac{P(t)}{\delta+P(t)}-m-m_1P(t)\right]dt\right). \end{aligned}$$

Since the initial conditions are non-negative, we can conclude that the solution of (1) is always non-negative.

The boundedness means that the populations of prey and predators are limited within certain boundaries. Ecological systems have finite resources, habitat capacities, and other constraints that impose limits on population growth. Boundedness ensures that the populations do not grow indefinitely but instead remain within realistic limits dictated by factors such as food availability, space, and interactions with other species. Using the first equation of (1), we see that

$$\begin{aligned} \frac{dN}{dt} &< rN\left(1-\frac{N}{k}\right),\\ \implies N(t) &< \frac{k}{1+kc_0e^{-rt}}. \end{aligned}$$

Hence, we see that $\lim_{t\to\infty}\sup N(t)<k$ which implies that the solution for prey density is bounded. Again to establish the boundedness of predator density, we consider the function $x(t)=N(t)+\frac{P(t)}{\epsilon}$ and differentiating both sides with respect to t by using the equation (1), we get

$$\begin{aligned} \frac{dx(t)}{dt}+\kappa x(t) &= (r+\kappa)N-\frac{rN^2}{k}-\frac{m_1P^2}{\epsilon}\\ &< \frac{k(r+\kappa)^2}{4r}\\ \implies x(t) &< \frac{k(r+\kappa)^2}{4r\kappa}, \end{aligned}$$

which implies that $x(t)$ is bounded and so both populations are bounded. It is clear from the above results that none of the populations grows infinitely.

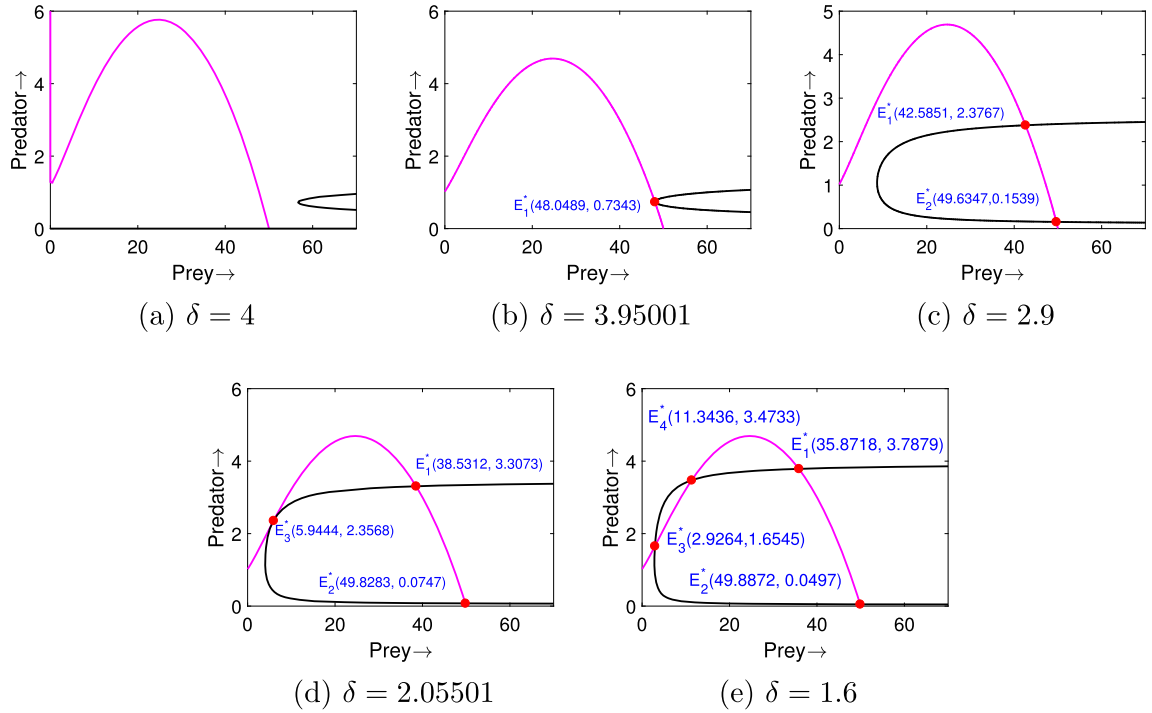

(a) $\delta = 4$ (b) $\delta = 3.95001$ (c) $\delta = 2.9$

(d) $\delta = 2.05501$ (e) $\delta = 1.6$

Fig. 2 Changing the number of equilibrium point(s) for different values of Allee effect(δ) and other parametric values are given in Table 2. Magenta and black curves are prey and predator nullcline, respectively

3.2 Equilibria of system (1)

The equilibria of the system (1) are solution of the following equations:

$$rN\left(1-\frac{N}{k}\right)-\frac{(\lambda+aP)NP}{1+h(\lambda+aP)N}=0, \tag{3}$$

$$\frac{\epsilon(\lambda+aP)NP}{1+h(\lambda+aP)N}\frac{P}{\delta+P}-mP-m_1P^2=0. \tag{4}$$

We get the following three types of equilibrium points:

(1) The trivial equilibrium point $E^0 = (0, 0)$. This equilibrium always exists. In this state, neither prey nor predator populations exist within the ecosystem.

(2) The predator-free axial equilibrium point $E^1 = (k, 0)$. This equilibrium is always present. In this state, only prey populations exist within the ecosystem.

(3) The interior equilibrium point $E^*(N^*, P^*)$, where $N^* = \dfrac{(P^*+\delta)(m+m_1P^*)}{(\lambda+aP^*)(\epsilon P^*-h(P^*+\delta)(m+m_1P^*))}$ and P^* is the root of the equation

$$AZ^6+BZ^5+CZ^4+DZ^3+EZ^2+FZ+G=0, \tag{5}$$

where the coefficients A, B, C, D, E, F, G are explicitly shown in Appendix A. This equilibrium holds ecological significance as it allows both prey and predator populations to coexist and survive.

According to the above analysis, the given system has at most six interior equilibrium points. In this case, it will be difficult to determine the number of interior equilibrium points analytically. We calculate equilibrium points numerically. For this purpose, we have considered the hypothetical values of the system parameters are shown in Table 2. The nullclines of the prey and predator populations of the model system (1) for different values of Allee effect δ are given in Fig. 2 and we see that maximum four interior equilibrium points exist which are denoted by $E_i^*(N^*, P^*)^*(i = 1-4)$.

Next, we examined how to change equilibrium points based on two parameters: $\lambda-\delta$ (see Fig. 3 (a)) and $a-\delta$ (see Fig. 3 (b), respectively. It is clear from Fig. 3 (a) that at higher values of δ, there is no interior equilibrium point. In this situation, only prey species can survive in the ecosystem. For moderate values of δ and any values of λ, two interior equilibria exist. Furthermore, for lower values of δ and higher values of λ the deterministic system (1) has four equilibria. Fig. 3 (b), for higher values of δ system does not have any interior equilibrium point. For moderate values of δ and higher values of a, the system has two interiors. For higher values of a and lower values of δ, the system has four interiors.

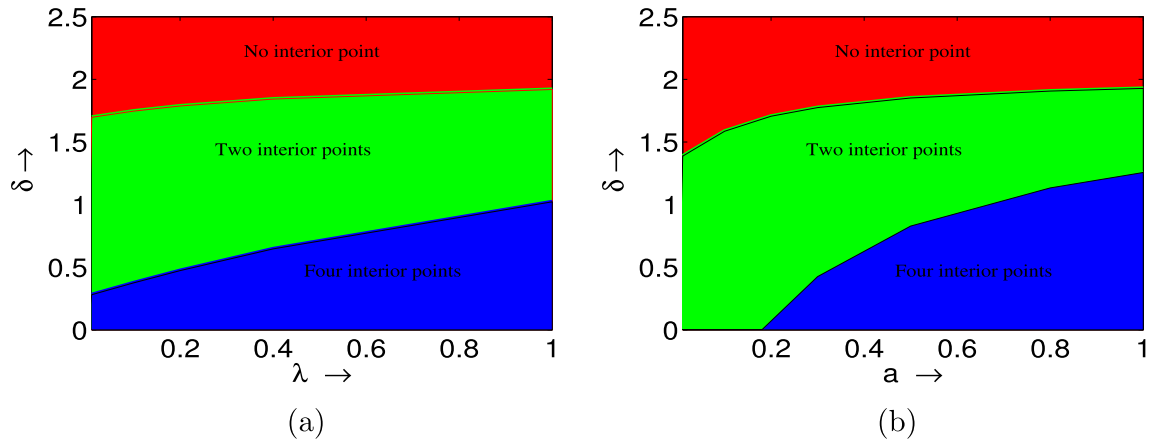

Fig. 3 Changing the number of interior equilibria shown in (a) $\lambda - \delta$ and (b) $a - \delta$ plane. Red, green, and blue color regions represent no interior, two interiors, and four interiors, respectively. All parameters are taken from Table 2 except $m = 0.1$

3.3 Stability of the equilibria

In this subsection, we shall discuss the stability of different types of equilibrium points. The Jacobian matrix $J_E(N,\ P)$ of the system (1) at any point $E(N, P)$ can be written as

$$\begin{pmatrix} r\left(1-\frac{2N}{k}\right)-\frac{P(\lambda+aP)}{(1+Nh(\lambda+aP))^2} & -\frac{N(\lambda+2Pa+Nh(\lambda+aP)^2)}{(1+Nh(\lambda+aP))^2} \\ \frac{\epsilon(\lambda+aP)P^2}{(1+Nh(\lambda+aP))^2(\delta+P)} & \frac{NP\epsilon(2\lambda+3aP)P^2}{(1+Nh(\lambda+aP))(\delta+P)}-\frac{NP^2\epsilon(\lambda+aP)(1+Nh(\lambda+a\delta+2Pa))}{(1+Nh(\lambda+aP))^2(\delta+P)^2}-m-2m_1P \end{pmatrix}. \quad (6)$$

Theorem 1 *The trivial equilibrium point E^0 is saddle and the axial equilibrium point E^1 is always stable.*

Proof The eigenvalues of the Jacobian matrix at E^0 are r and $-m$. Since the eigenvalues are opposite in sign and so the trivial equilibrium point E^0 is always saddle. Also, the eigenvalues of E^1 are $-r$ and $-m$. Since both eigenvalues are negative and so the axial equilibrium point is always stable. Hence the proof. □

Biologically, above two findings are important because the first result implies that both populations will not extinct simultaneously but the second result implies predator extinction is probable. For the survival of both populations, there must exist bistability in this biological system.

For the interior equilibrium point $E^*(N^*,\ P^*)$ the Jacobian matrix can be expressed as $J_{E^*}(N^*,\ P^*) = \begin{pmatrix} a_{11} & a_{12} \\ a_{21} & a_{22} \end{pmatrix}$, where a_{11}, a_{12}, a_{21}, a_{22} are given in Appendix B. The eigenvalues of the matrix $J_{E^*}(N^*,\ P^*)$ are determined by the equation

$$\lambda^2 - c\lambda + d = 0, \quad (7)$$

where $c = Trace(J_{E^*}(N^*,\ P^*)) = a_{11}+a_{22}$ and $d = det(J_{E^*}(N^*,\ P^*)) = a_{11}a_{22}-a_{21}a_{12}$. The stability of the interior equilibrium point $E^*(N^*,\ P^*)$ depend on the following cases:

(1) If $c < 0, d > 0$ then E^* is a stable equilibrium point and if $c^2 - 4d \geq 0$ then it is a stable node otherwise it is a stable spiral.
(2) If $d < 0$ then E^* is saddle point.
(3) If $c > 0, d > 0$ then E^* is an unstable equilibrium point and if $c^2 - 4d \geq 0$ then it is an unstable node otherwise it is an unstable spiral.

Since it is quite challenging to determine the expression of the interior equilibrium point analytically, the above analysis cannot be performed accurately. We use the geometric approach to study interior equilibrium points [46].

3.3.1 Geometric approach for stability criteria

In the above subsection, we discuss the theoretical conditions for the stability of the interior equilibrium points. In this subsection, we demonstrate the geometrical approach for the stability of the interior equilibrium point. For the interior equilibrium point $E^*(N^*, P^*)$ the Jacobian matrix can be expressed as

$$J_{E^*}(N^*,\ P^*) = \begin{pmatrix} N^*\frac{\partial f}{\partial N} & N^*\frac{\partial f}{\partial P} \\ P^*\frac{\partial g}{\partial N} & P^*\frac{\partial g}{\partial P} \end{pmatrix}.$$

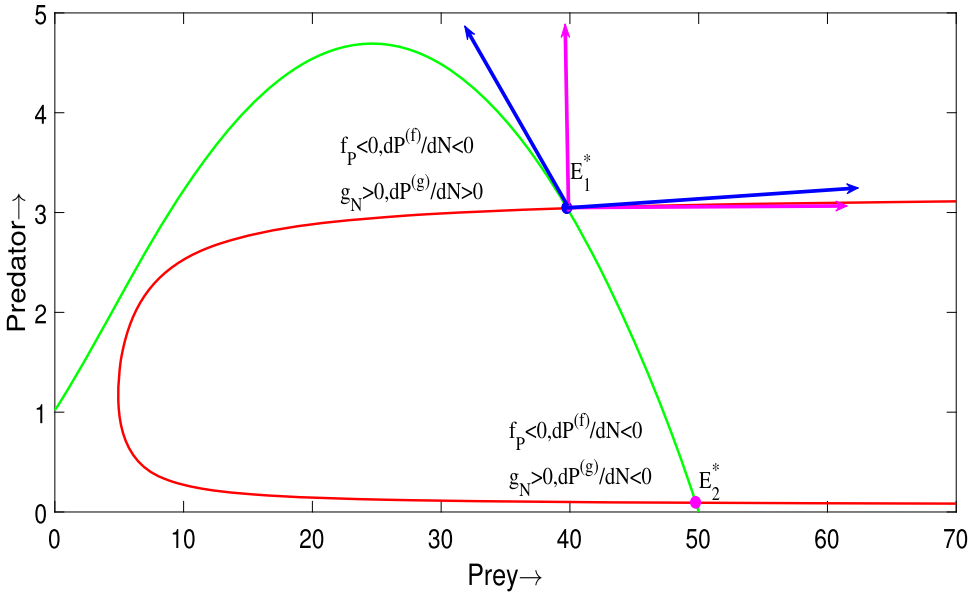

Fig. 4 Green and red curves are prey and predator nullcline, respectively. The figure shows the geometric approach for the stability of the interior equilibrium point for $\delta = 2.3$, $a = 0.6$. Magenta and blue lines are the axes and corresponding tangent lines at E^*. Remaining other parametric values are given in Table 2

We consider the formula $\frac{dP^{(f)}}{dN} = -\frac{f_N}{f_P}$ and $\frac{dP^{(g)}}{dN} = -\frac{g_N}{g_P}$, then from above we get

$$J_{E^*}(N^*,\ P^*) = \begin{pmatrix} -N^*\frac{\partial f}{\partial P}\frac{dP^{(f)}}{dN} & N^*\frac{\partial f}{\partial P} \\ P^*\frac{\partial g}{\partial N} & -\frac{P^*\frac{\partial g}{\partial N}}{\frac{dP^{(g)}}{dN}} \end{pmatrix}.$$

Furthermore, we have seen that

$$\frac{\partial f}{\partial N} = -\frac{r}{k} + \frac{r^2 h}{p^*}\left(1 - \frac{N^*}{k}\right)^2,\ \frac{\partial f}{\partial P} = -\left[\frac{\lambda + 2aP^* + hN^*(\lambda + aP^*)^2}{(1 + N^*h(\lambda + aP^*))^2}\right] < 0$$
$$\frac{\partial g}{\partial N} = \frac{\epsilon P h(\lambda + aP)}{h(\delta + P)(1 + Nh(\lambda + aP))^2} > 0,\ \frac{\partial g}{\partial P} = \frac{m + m_1 P^*}{P^*(\delta + P^*)} - \frac{a\epsilon P^* N^*}{(1 + N^*h(\lambda + aP^*))^2(\delta + P^*)} - m_1.$$

(1) From Fig. 4, it is clear that $\frac{dP^{(f)}}{dN} < 0$ (since the slope of the tangent line at E^* is negative) and $\frac{dP^{(g)}}{dN} > 0$. So the sign of each element of the jacobian matrix at the interior equilibrium point is $\begin{pmatrix} - & - \\ + & - \end{pmatrix}$. It is clear that the $Det(J_{E^*}(N^*,\ P^*)) > 0$ and $Trace(J_{E^*}(N^*,\ P^*)) < 0$ so the interior equilibrium point is stable in nature. Using this approach, we can discuss two and four interior equilibria, and the remaining equilibria can be discussed similarly.

(2) From Fig. 2(c), it is already discuss from previous part that $sign(J_{E_1^*}(N^*,\ P^*)) = \begin{pmatrix} - & - \\ + & - \end{pmatrix}$ and so E_1^* is stable. Again for the equilibrium E_2^*, we see (Fig. 4) that along the predator nullcline the gradient of the tangent line is negative, i.e., $\frac{dP^{(g)}}{dN} < 0$. So $sign(J_{E_2^*}(N^*,\ P^*)) = \begin{pmatrix} - & - \\ + & + \end{pmatrix}$. Therefore, we cannot conclude that this interior equilibrium point is stable. But since one of the interior equilibrium points is stable and so another cannot be stable.

(3) Also from Fig. 2(e), it is clear that there exist four interior equilibria. Using the same technique as above, we say that E_1^* is stable. We cannot conclude the stability using the geometric approach for E_2^* and it will depend on the sign of determinant and trace of the corresponding jacobian matrix. For the equilibrium point, E_3^* we see both the curve is increasing in the neighborhood of E_3^*. So the sign of elements of the Jacobian matrix are $\begin{pmatrix} + & - \\ + & + \end{pmatrix}$. This implies that E_3^* must be unstable. Using the same reason as for E_3^* we say that E_4^* is unstable.

3.4 Bifurcation analysis

This subsection discusses different types of bifurcation analysis for different parameter values. Bifurcation means the change in the qualitative behaviour of solutions with respect to the stable-instable nature or number of equilibrium point(s).

3.5 Study of creation and destroy of equilibrium points through saddle-node bifurcation

We rewrite the given system in the following form,

$$\dot{X} = \begin{pmatrix} f(N,P) \\ g(N,P) \end{pmatrix} = F(N,P), \tag{8}$$

where $X = \begin{pmatrix} N \\ P \end{pmatrix}$. Fixing other parameters if we consider r as the bifurcation parameter then it is possible to find a critical value $r = r^{[s]}$ such that both roots of (5) will coincide. In this situation, one of the characteristic roots $J_{E^*}(N^*,\ P^*)$ vanishes. To discuss this bifurcation, we use Sotomayor theorem [47].

Theorem 2 *The system (1) execute saddle node bifurcation at coincide interior equilibrium point $E^*(N^*,\ P^*)$ at $r = r^{[s]}$ if* $a_{21}\left(a_{12}^2 f_{NN} - 2a_{12}a_{11}f_{NP} + a_{11}^2 f_{PP}\right) \neq a_{11}\left(a_{12}^2 g_{NN} - 2a_{12}a_{11}g_{NP} + a_{11}^2 g_{PP}\right)$.

Proof Let V_1 and W_1 be the eigenvectors corresponding to the eigenvalue 0 for the matrix $J_{E^*}(N^*,\ P^*)$ and transpose of it, then $V_1 = \begin{pmatrix} a_{12} \\ -a_{11} \end{pmatrix}$ and $W_1 = \begin{pmatrix} a_{21} \\ -a_{11} \end{pmatrix}$. We have $F_r(E^*(N^*,\ P^*)) = \begin{pmatrix} N^*\left(1 - \frac{N^*}{k}\right) \\ 0 \end{pmatrix}$, which gives $W_1^T F_r(E^*(N^*,\ P^*)) = a_{21}N^*\left(1 - \frac{N^*}{k}\right) \neq 0$. So $W_1^T D^2 F(E^*(N^*,\ P^*))(V,\ V) = a_{21}\left(a_{12}^2 f_{NN} - 2a_{12}a_{11}f_{NP} + a_{11}^2 f_{PP}\right) - a_{11}\left(a_{12}^2 g_{NN} - 2a_{12}a_{11}g_{NP} + a_{11}^2 g_{PP}\right) \neq 0$. The explicit expression of a_{ij} and different derivatives of f and g are given in Appendix B and C. Hence we conclude from Sotomayor theorem [47] that the system undergoes to saddle-node bifurcation at interior equilibrium point. □

3.6 Study of existence of periodic solution through Hopf bifurcation

Theorem 3 *The system undergoes Hopf bifurcation at an interior equilibrium point $E^*(N^*,\ P^*)$ at $r = r^{[H]}$.*

Proof We assume $r^{[H]}$ in such a way that at $r = r^{[H]}$, $det(J_{E^*}(N^*,\ P^*)) > 0$ and $Trace(J_{E^*}(N^*,\ P^*)) = 0$. Then we conclude that the characteristic equation (7) has a purely imaginary root. Also, we see that the transversality condition $\frac{\partial}{\partial r}(Trace(J_{E^*}(N^*,\ P^*))) = 1 - \frac{2N^*}{k} \neq 0$ hold. Hence to find the Lyapunov number and stability of the limit cycle, we consider the following transformation:

$$N = \bar{N} + N^* \text{ and } P = \bar{P} + P^*.$$

using the above transformation the system (1) changes as follows:

$$\dot{\bar{N}} = \alpha_{10}\bar{N} + \alpha_{01}\bar{P} + \alpha_{20}\bar{N}^2 + \alpha_{11}\bar{N}\bar{P} + \alpha_{02}\bar{P}^2 + \alpha_{30}\bar{N}^3 + \alpha_{21}\bar{N}^2\bar{P} + \alpha_{12}\bar{N}\bar{P}^2 + \alpha_{03}\bar{P}^3 + \ldots\ldots \tag{9}$$

$$\dot{\bar{P}} = \beta_{10}\bar{N} + \beta_{01}\bar{P} + \beta_{20}\bar{N}^2 + \beta_{11}\bar{N}\bar{P} + \beta_{02}\bar{P}^2 + \beta_{30}\bar{N}^3 + \beta_{21}\bar{N}^2\bar{P} + \beta_{12}\bar{N}\bar{P}^2 + \beta_{03}\bar{P}^3 + \ldots\ldots \tag{10}$$

where, $\alpha_{10} = a_{11}$, $\alpha_{01} = a_{12}$, $\alpha_{20} = f_{NN}$, $\alpha_{11} = f_{NP}$, $\alpha_{02} = f_{PP}$, $\alpha_{30} = f_{NNN}$, $\alpha_{21} = f_{NNP}$, $\alpha_{12} = f_{NPP}$, $\alpha_{03} = f_{PPP}$ and $\beta_{10} = a_{21}$, $\beta_{01} = a_{22}$, $\beta_{20} = g_{NN}$, $\beta_{11} = g_{NP}$, $\beta_{02} = g_{PP}$, $\beta_{30} = g_{NNN}$, $\beta_{21} = g_{NNP}$, $\beta_{12} = g_{NPP}$, $\beta_{03} = g_{PPP}$, The explicit expression of the derivative of f and g and other coefficients are given in Appendix B and C and some of them are removed for their large expression. At $r = r^{[H]}$ the following conditions hold :

$$\alpha_{10} + \beta_{01} = 0 \text{ and } \alpha_{10}\beta_{01} - \beta_{10}\alpha_{01} > 0.$$

Let there exit a neighbourhood of $r^{[H]}$ say $(r^{[H]} - \epsilon_1,\ r^{[H]} + \epsilon_1)$, $\epsilon_1 > 0$ in which eigenvalues of the $J_{E^*}(N^*,\ P^*)$ be complex conjugate i.e., of the form $a(r) \pm ib(r)$ and we take the transformation $\xi_1 = \bar{N}$, $\xi_2 = \frac{a(r) - \alpha_{10}}{\alpha_{01}}\bar{N} + \frac{b(r)}{\alpha_{01}}\bar{P}$ then the above system (9) reforms as

$$\dot{\xi_1} = a(r)\xi_1 - b(r)\xi_2 + \phi_1(\xi_1, \xi_2) \tag{11}$$

$$\dot{\xi_2} = b(r)\xi_1 + a(r)\xi_2 + \phi_2(\xi_1, \xi_2) \tag{12}$$

Table 2 Parameters value for the deterministic model (1)

r	k	λ	a	h	ϵ	δ	m	m_1
0.81	50	0.18	0.31	0.45	0.28	1.35	0.01	0.11

where, $\phi_1(\xi_1, \xi_2) = k_{20}\xi_1^2 + k_{11}\xi_1\xi_2 + k_{02}\xi_2^2 + k_{30}\xi_1^3 + k_{21}\xi_1^2\xi_2 + k_{12}\xi_1\xi_2^2 + k_{03}\xi_2^3$..... and $\phi_2(\xi_1, \xi_2) = l_{20}\xi_1^2 + l_{11}\xi_1\xi_2 + l_{02}\xi_2^2 + l_{30}\xi_1^3 + l_{21}\xi_1^2\xi_2 + l_{12}\xi_1\xi_2^2 + l_{03}\xi_2^3$..... The expression of k_{ij} and l_{ij} are given in Appendix D. Applying polar transformation [48–50] the above system reforms as

$$\dot{r} = a(r)r + \sigma_1(r)r^3 + ...$$
$$\dot{\theta} = b(r) + \sigma_2(r)r^2 + ...$$

Let us apply Taylor's expansion of the above normal form w.r.t $r = r^{[H]}$ and we get,

$$\dot{r} = a^{'}(r^{[H]})(r - r^{[H]})r + \sigma_1(r^{[H]})r^3 + ...$$
$$\dot{\theta} = b(r^{[H]}) + (r - r^{[H]})b^{'}(r^{[H]}) + \sigma_2(r^{[H]})r^2 + ...$$

In the above expression, the coefficient of r^3 is the first Lyapunov constant (σ_1) and its expression in simplified form is given bellow [51]

$$\sigma_1 = \frac{1}{16}[(\phi_{1\xi_1\xi_1\xi_1} + \phi_{1\xi_1\xi_2\xi_2} + g_{\xi_1\xi_1\xi_2} + \phi_{2\xi_2\xi_2\xi_2}) + \frac{1}{b(r^{[H]})}\{\phi_{1\xi_1\xi_2}(\phi_{1\xi_1\xi_1} + \phi_{1\xi_1\xi_1}) - \phi_{2\xi_1\xi_2}(\phi_{2\xi_1\xi_1} + \phi_{2\xi_2\xi_2}) - \phi_{1\xi_1\xi_1}\phi_{2\xi_1\xi_1} + \phi_{1\xi_2\xi_2}\phi_{2\xi_2\xi_2}\}]_{(\xi_1=0,\xi_2=0,r=r^{[H]})}. \quad (13)$$

The Hopf bifurcation theorem [52] states if $\sigma_1 > 0$ then the system exhibit subcritical Hopf bifurcation and if $\sigma_1 < 0$ then it exhibit supercritical hopf bifurcation. □

4 Numerical simulation for deterministic model

In this part, we shall discuss the numerical results of the system (1) with the help of MAPLE, MATLAB software. To conduct numerical simulations of the deterministic model (1), we utilized parameter values listed in Table 2, sourced from previous publications [41, 53].

In Fig. 5, we have presented a one-parameter bifurcation diagram with respect to r, k, λ, and δ. It is clear from Figs. 5($a - c$) that with the increase the values of r, k, and λ the deterministic system (1) becomes unstable with stable limit cycle. Also the radius of the limit cycle increase with increasing the values of parameters r, k, and λ. Also, another scenario observes for the parameter δ. If we increase the parameter δ then the solution becomes stable (see Fig. 5 (d)). The radius of the stable limit cycle is decreasing as increasing the parameter δ and it goes to zero for $\delta > 2$.

For a better understanding of the complex dynamics of the deterministic model (1), we draw a one-parameter bifurcation diagram ($N-$ component solution curves for interior equilibrium point(s) with their nature) for different parameters and also drawn the corresponding phase portrait depending the nature of the interior equilibrium point(s) (see Figs. 6-9). At first, we plot a one-parameter bifurcation diagram (see Fig. 6) where k is the bifurcation parameter. It is clear from Fig. 6, for lower values of k, the deterministic system has no interior, and increasing values of k, the system has two interiors, one stable and one saddle in nature, i.e., the deterministic system experiences saddle-node bifurcation. Again increasing the values of k the stable interior becomes unstable with a stable limit cycle and other equilibrium points have the same nature, i.e., the deterministic model (1) experiences Hopf bifurcation. There are two more interiors in the system with increasing k values, one of which is stable other one is a saddle, and the rest are the same, i.e., the system again experiences the saddle-node bifurcation. As k is increased, the system experiences saddle-node bifurcation, such that there are only two interiors, saddle, and stable. The corresponding phase portrait is shown in Fig. 6. It is clear from the above discussion that the deterministic model (1) exhibits complex dynamics with carrying capacity (k).

Next, we pick the parameter λ, and plot the bifurcation diagram of the deterministic model (1) (see Fig. 7). It is apparent from the figure that up to a certain value of λ, the deterministic model (1) exhibits two interior equilibria. Out of which, one is always saddle while another one is stable. On boosting up the value of λ, we see that the deterministic model (1) experiences a saddle-node bifurcation, and there is a range of λ for which the model (1) exhibits four interior equilibria. These four interior equilibria are of different features; two are saddle, one is unstable and one is stable. We observed that furthermore increment in the value of λ leads to another saddle-node bifurcation in the system (1), and after the threshold value of λ, the system (1) again exhibits two interior equilibria. The figure clearly shows that one of the two interior equilibria is saddle whereas the second one is unstable, here only prey can survive in the system because none of the interiors are stable or stable limit cycles. In Fig. 7, we see that our model (1) undergoes saddle-node bifurcation twice when λ is increased.

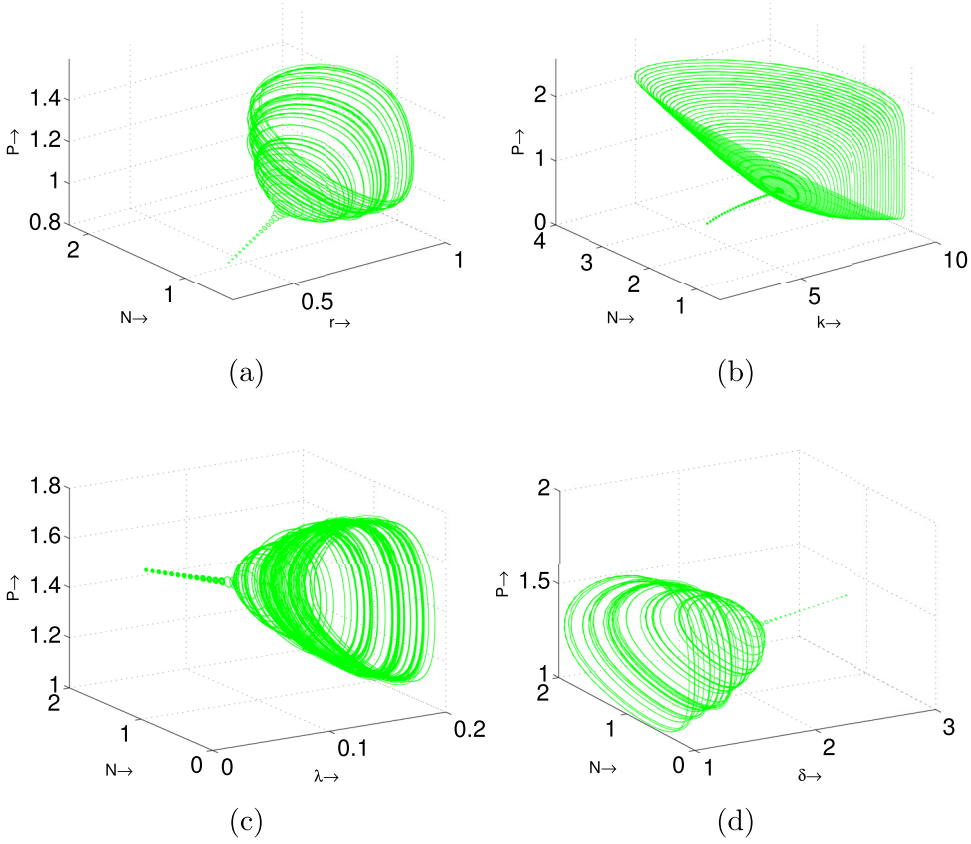

Fig. 5 The bifurcation diagram of the system (1) with respect to (a) r, (b) k, (c) λ, (d) δ and rest of parameters are taken from Table 2 except in (a), (c), (d), $k = 5$

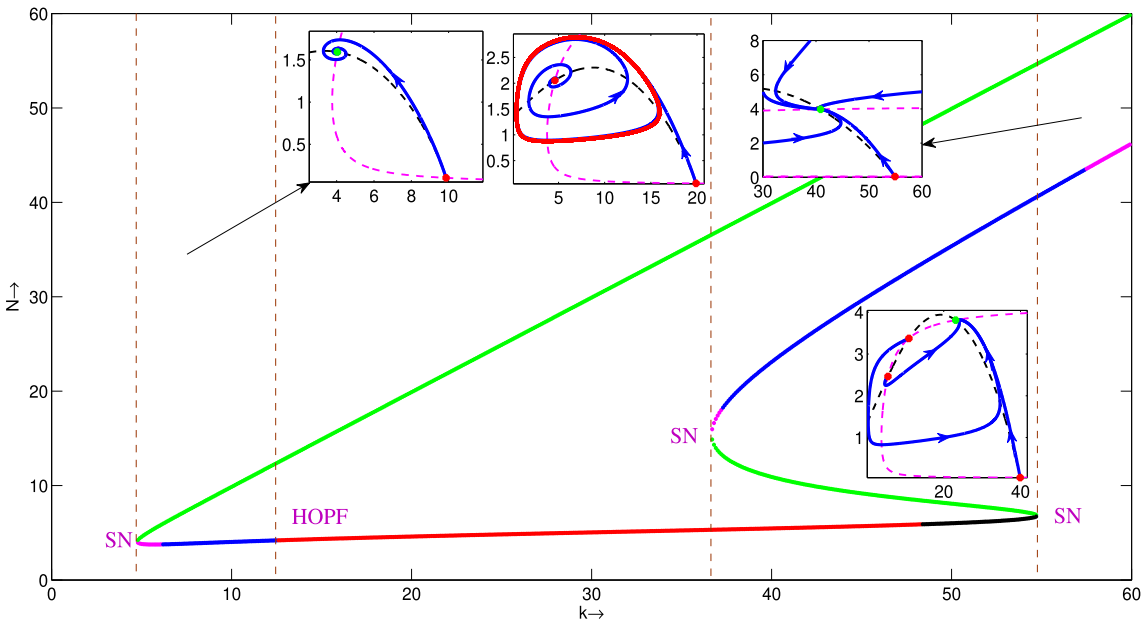

Fig. 6 Solution curve for interior equilibrium point(s) with their nature and the corresponding phase portrait with respect to k. Blue and magenta color curves represent stable spiral and stable node, respectively. The red and black color curves represent an unstable spiral and unstable node, respectively whereas the green color curve represents a saddle in nature. The rest of the parameters are taken from Table 2

Next, in Fig. 8, we vary the parameter a to see the dynamics of the deterministic system (1). The figure shows that if a is below a fixed value, then the deterministic system (1) exhibits two interior equilibria: one saddle and another stable. We observed that on increasing the value of parameter a, the dynamics of the system (1) changes drastically. There is a threshold value of a at which the system passes through a saddle-node bifurcation and for a range of a, it exhibits four interior equilibria. We find that two interior

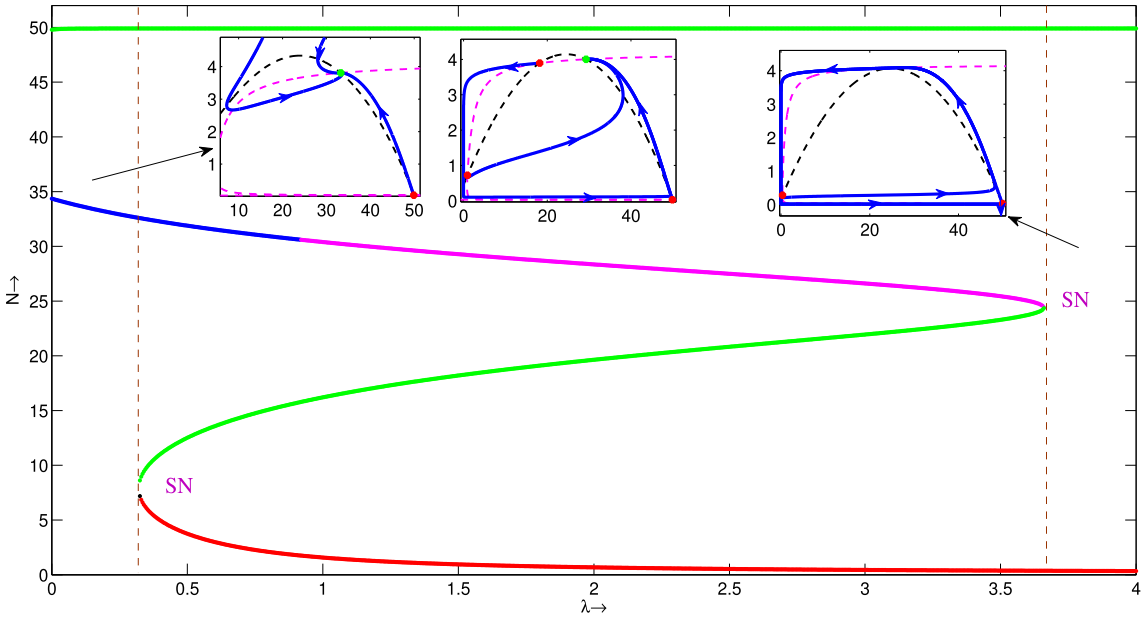

Fig. 7 Solution curve for interior equilibrium point(s) with nature and the corresponding phase portrait with respect to λ. Blue and magenta color curves represent stable spiral and stable node, respectively. The red and black color curves represent an unstable spiral and unstable node, respectively whereas the green color curve represents a saddle in nature. The rest of the parameters are taken from Table 2 except $r = 0.71$ and $a = 0.2$

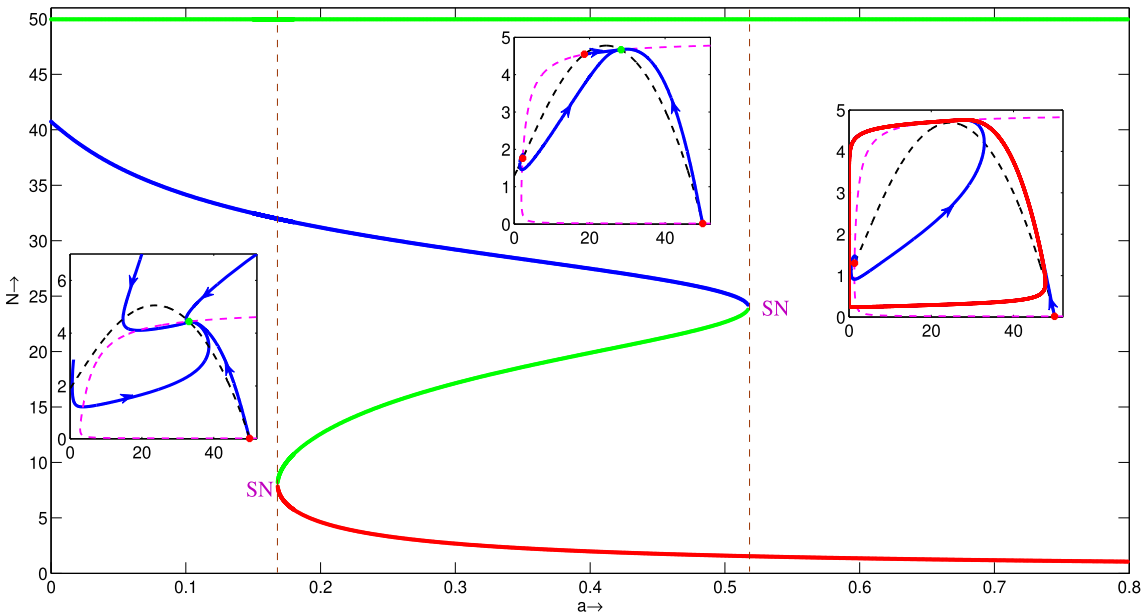

Fig. 8 Solution curve for interior equilibrium point(s) with nature and the corresponding phase portrait with respect to a. Blue and magenta color curves represent stable spiral and stable node, respectively. The red and black color curves represent an unstable spiral and unstable node, respectively whereas the green color curve represents a saddle in nature. Rest of parameters are taken from Table 2 except $\delta = 0.65$

equilibria are saddle, one is unstable while one is stable. Moreover, we observe another saddle-node bifurcation in the system if a surpasses a critical value. System (1) is now found to exhibit two interior equilibria among them one is a saddle and another one is an unstable spiral with a stable limit cycle. Thus, Fig. 8 depicts complex dynamics of the system (1) for the cooperation coefficient.

In Fig. 9, we plot the bifurcation diagram of the system (1) by varying the parameter δ. The figure shows that for lower values of δ, the system (1) exhibits two interior equilibria; one of which is a saddle while the other is an unstable spiral with a stable limit cycle. On increasing the value of δ, we find that system (1) exhibits four interior equilibria and there is a saddle-node bifurcation of the equilibrium points. Of the four equilibrium points, one is stable, one is unstable and two are saddle. We again observe the appearance of saddle-node bifurcation and the system (1) exhibits two interior equilibria after another threshold value of λ. Deterministic system (1) experiences one more saddle-node bifurcation for λ, and after that critical value of λ, the system does not have any interior

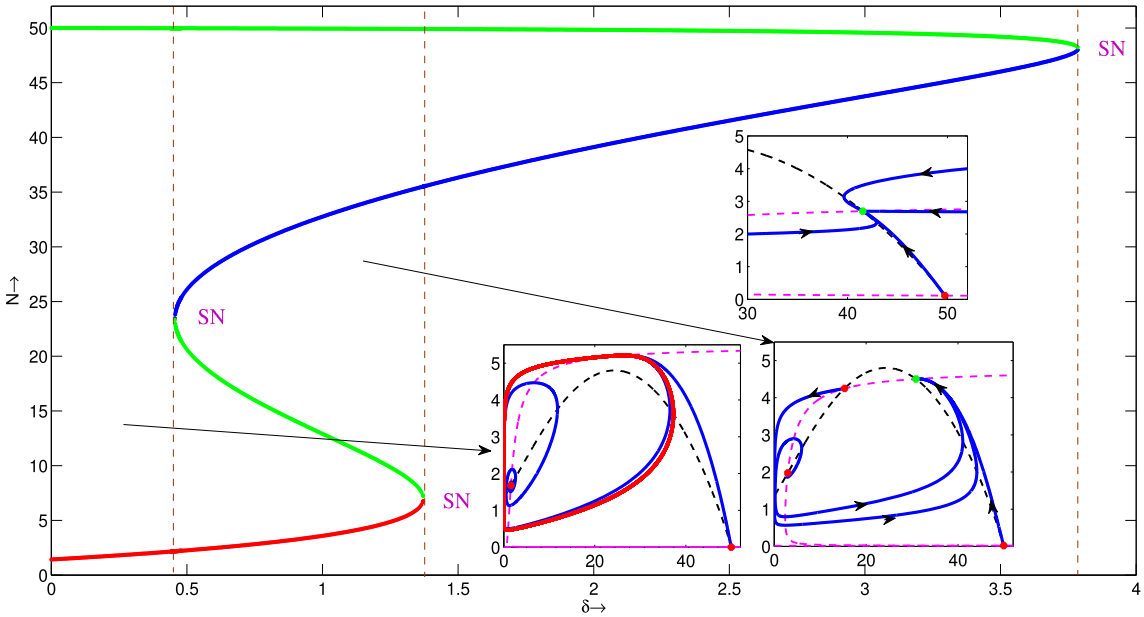

Fig. 9 Solution curve for interior equilibrium point(s) with nature and the corresponding phase portrait with respect to δ. Blue and magenta color curves represent stable spiral and stable node, respectively. The red and black color curves represent an unstable spiral and unstable node, respectively whereas the green color curve represents saddle in nature. Rest of parameters are taken from Table 2

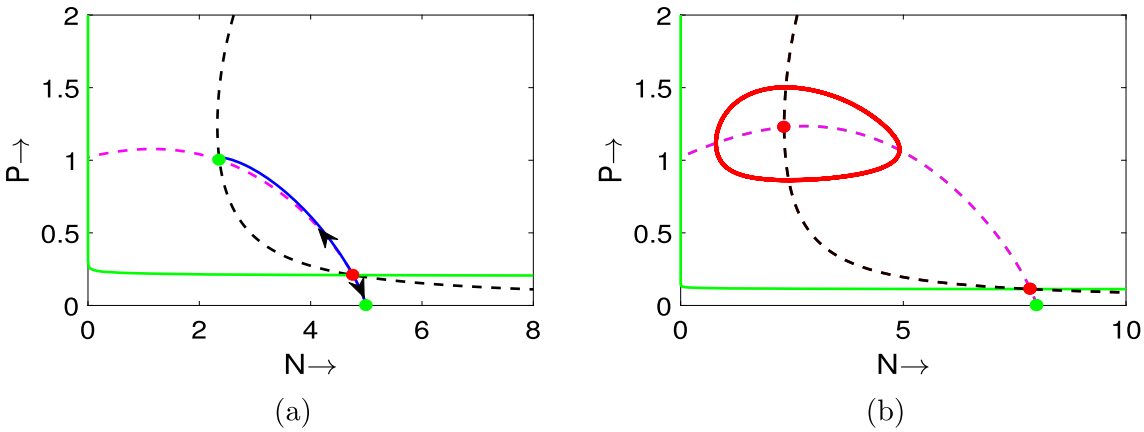

Fig. 10 Basin of attraction of the interior and axial equilibrium point. Green curve represents sepatrix. All parameters are taken from Table 2 except $a = 0.6$ and in (a) $k = 5$ and in (b) and $k = 8$

equilibrium, in this scenario the prey species only survive in the system. It is clear from Fig. 9 and Fig. 5 (d) that for $\delta = 0$, the system is showing oscillatory behaviour with a limit cycle. But increasing δ towards moderate values the limit cycle disappears through saddle-node bifurcation and a stable interior equilibrium point arises. For higher values of δ the predator population goes to extinction (i.e., the interior equilibrium point disappears) through another saddle-node bifurcation.

We have to note that in Figs. 6-9 the system shows bi-stable nature when the interior equilibrium point is stable or stable limit cycle arises around it. The bi-stability occurs because the axial equilibrium point is always stable (see Fig. 10). In these cases, the coexistence of both species not only depends on parameter values but also on initial population density.

We now plot a bifurcation diagram when two parameters are changed simultaneously (see Fig. 11 (a) and (b)). It is clear from Fig. 11 (a) and (b) that r has tendency to stabilized the system but λ and a are both destabilized the system.

5 Mathematical analysis of stochastic model

In this section, we discuss the stochastic model (2) of the prey-predator system (1). At first, we will show the existence and uniqueness of the solution, stationary distribution, and then the extinction and persistence of the solution. The theoretical result is also validated by numerical simulation.

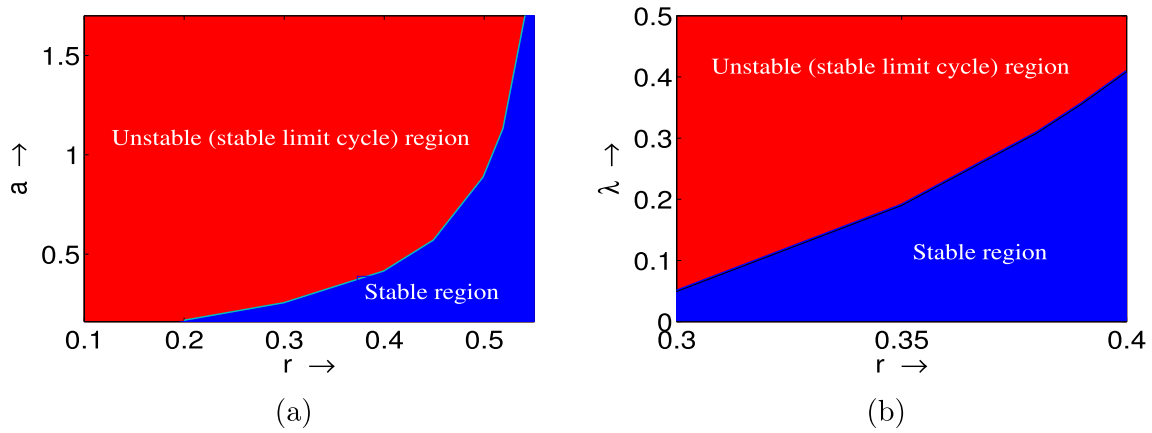

Fig. 11 This figure display the Hopf bifurcation curve in (*a*) $r - a$ plane and in (*b*) $r - \lambda$. All parameters are taken from Table 2 except $a = 0.2$

Notations: Let us consider the stochastic differential equation in the following form

$$dX(t) = a(X)dt + \sum_{k=1}^{2} \sigma_k(X) dB_k(t), \; X(0) = X_0 \tag{14}$$

where $X(t)$ denotes a Markov process, $B_k(t)$ represents standard Brownian motion of dimension 2. Then the diffusion matrix $A(X)$ of $X(t)$ can be expressed as $A(X) = (a_{ij}(X))$, where $(a_{ij}(X)) = \sum_{k=1}^{2} \sigma_k^i(X)\sigma_k^j(X)$.

5.1 Uniqueness and existence of global positive solution

For the uniqueness of a global positive solution of the stochastic differential equation, the involved function in the stochastic system is needed to hold the linear growth condition and local Lipschitz condition [54–56]. Since the stochastic system (2) does not satisfy the linear growth condition and so the solution of the system may explode at a finite time. So we consider the following theorem.

Theorem 4 *The system (2) has a unique positive global solution (N(t), P(t)) for any initial values of* $(N(0),\ P(0)) \in \mathbb{R}^2_+$ *for all* $t \in [0,\ \tau_e)$ *almost surely (a.s) if* $m_1 > a$. *Also, the solution remains in* $\mathbb{R}^2_+$ *with probability 1, where* τ_e *is the explosion time.*

Proof Let us consider the following transformation $x(t) = \ln(N(t))$, $y(t) = \ln(P(t))$ and using the Ito's formula [55] the system (2) reforms as follows:

$$dx(t) = \left[r\left(1 - \frac{e^{x(t)}}{k}\right) - \frac{(\lambda + ae^{y(t)})e^{y(t)}}{1 + h(\lambda + ae^{y(t)})e^{x(t)}} - \frac{\sigma_1^2}{2} \right] dt + \sigma_1 dB_1(t),$$

$$dy(t) = \left[\frac{\epsilon(\lambda + ae^{y(t)})e^{x(t)}}{1 + h(\lambda + ae^{y(t)})e^{x(t)}} \frac{e^{y(t)}}{\delta + e^{y(t)}} - m - m_1 e^{y(t)} - \frac{\sigma_2^2}{2} \right] dt + \sigma_2 dB_2(t).$$

Here is the initial condition $x(0) = \ln(N(0))$, $y(0) = \ln(P(0))$ and it is clear that the corresponding stochastic function of the above system satisfies the local Lipschitz condition. Then $N(t) = e^{x(t)}$ and $P(t) = e^{y(t)}$ are the local positive solution of system (2). In the next step, we show that the solution is global and so we choose a non-negative integer k_0 such that $N(0)$, $P(0)$ lies within the interval $\left[\frac{1}{k_0},\ k_0\right]$. We define the stopping time τ_k for any integer $k > k_0$ as follows:

$$\tau_k = \inf\left\{ t \in [0,\ \tau_e) : N(t) \notin \left(\frac{1}{k},\ k\right) \text{ or } P(t) \notin \left(\frac{1}{k},\ k\right) \right\}.$$

It is clear that τ_k is increasing function for $k \to \infty$. Let $\lim_{k\to\infty} = \tau_\infty$ whence $\tau_\infty \le \tau_e$. To show that the solution is global we have to show $\tau_e = \infty$ which is equivalent to showing $\tau_\infty = \infty$. We use the method of contradiction to prove it. Let us assume that the statement is false and so there exists $M > 0$ and $\epsilon \in (0,\ 1)$ such that $P(\tau_\infty \le M) > \epsilon$. So there exists a constant $p_1 > p_0$ for which $P(\tau_p \le M) \ge \epsilon$ for all $p \ge p_1$. Let us define $V(N,\ P) = N + 1 - \ln N + P + 1 - \ln P$. Using Ito's formula and we get

$$dV = (N-1)\left[r\left(1 - \frac{N}{k}\right) - \frac{(\lambda + aP)P}{1 + h(\lambda + aP)N} + \frac{\sigma_1^2}{2} \right] dt + (P - 1)$$

$$\begin{aligned}
&\left[\frac{\epsilon(\lambda+aP)N}{1+h(\lambda+aP)N}\frac{P}{\delta+P}-m-m_1P+\frac{\sigma_2^2}{2}\right]dt+\sigma_1(N-1)dB_1(t)+\sigma_2(P-1)dB_2(t)\\
&\leq\left[\frac{Nr(k+1)}{k}-(m_1-a)P^2+\left(\lambda-m+m_1+\frac{\epsilon}{h}\right)P+m\right]dt\\
&\quad+\sigma_1(N-1)dB_1(t)+\sigma_2(P-1)dB_2(t)\\
&\leq\left[\frac{Nr(k+1)}{k}+\left(\lambda-m+m_1+\frac{\epsilon}{h}\right)P+m\right]dt\\
&\quad+\sigma_1(N-1)dB_1(t)+\sigma_2(P-1)dB_2(t)\quad[\text{since } m_1>a]\\
&\leq 2\left[\left(\frac{r(k+1)}{k}\right)(N+1-\ln N)+2\left(\lambda+m_1+\frac{\epsilon}{h}\right)(P+1-\ln P)+m\right]\\
&\quad+\sigma_1(N-1)dB_1(t)+\sigma_2(P-1)dB_2(t)\\
&\qquad[\text{using the inequality } z_i\leq 2(z_i+1-\ln z_i)].
\end{aligned}$$

Let $C=\max\left\{\frac{2r(k+1)}{k},\ 2\left(\lambda+m_1+\frac{\epsilon}{h}\right),\ m\right\}$, then from above we get

$$dV\leq C(V+1)dt+\sigma_1(N-1)dB_1(t)+\sigma_2(P-1)dB_2(t).$$

So from integrating both sides from 0 to $\tau_k\wedge M$ with Ito's integral formula [57] and taking exception by using Grownwall's inequality [55] we get,

$$\begin{aligned}
EV(N(\tau_k\wedge M),\ P(\tau_k\wedge M))&\leq V(N(0),\ P(0))+CE\int_0^{\tau_k\wedge M}(V+1)dt\\
&\leq V(N(0),\ P(0))+CM+C\int_0^{\tau_k\wedge M}EV(N,\ P)dt\\
&\leq[V(N(0),\ P(0))+CM]e^{CM}\\
&=M_1.
\end{aligned}$$

Hence $V(N(\tau_k\wedge M),\ P(\tau_k\wedge M))\geq(k-1-\ln k)\wedge\left(\frac{1}{k}-1-\ln\frac{1}{k}\right)$. So it can be easily derived that $M_1\geq E[1_{\Omega_t}(\theta)V(N(\tau_k\wedge M),\ P(\tau_k\wedge M))]\geq\epsilon\left[(k-1-\ln k)\wedge\left(\frac{1}{k}-1-\ln\frac{1}{k}\right)\right]$, where 1_{Ω_t} is the indicator function of Ω_t. Letting $k\to\infty$, we get $\infty>M_1=\infty$ which is a contradiction. This completes the proof. □

5.2 Existence of stationary distribution

In this subsection, we show the existence of stationary distribution in (2). Here stationary distribution implies it is a stationary Markov process. In this case, both the populations are persistent and extinction cannot occur. The existence of stationary distribution gives the stability of the solution in a stochastic sense.

Lemma 1 *Let g(.) be a functional integrable about the measure μ. If the following conditions hold:*

(1) The smallest eigenvalue of the diffusion matrix bounded away from zero in the bounded domain $U\subset E_l$ with regular boundary and some neighborhood thereof.
(2) If $x\in E_l\backslash U$, the mean time τ_1 at which a path emerging from x reaches the set U is finite and $\sup_{x\in V}E_x\tau_1<\infty$ for every compact subset $V\subset E_l$.

Then the Markov process X(t) has a stationary distribution $\mu(.)$. Also

$$P_x\left\{\lim_{T\to\infty}\frac{1}{T}\int_0^T g(X(t))dt=\int_{E_l}g(x)\mu(dx)\right\}=1.$$

Theorem 5 *Let* $m_1>\frac{\epsilon}{P^*+\delta}$, $\beta<\min\left\{\left(\frac{r}{k}\right)N^{*2},\ \left(m_1-\frac{\epsilon}{P^*+\delta}\right)\left(P^*-\frac{(1+\epsilon)(\delta+P^*)}{2h(m_1P^*-m_1\delta-\epsilon)}\right)^2\right\}$, *where* $\beta=\frac{(1+\epsilon)^2(\delta+P^*)}{4h^2(m_1P^*-m_1\delta-\epsilon)}+\frac{2(1+\epsilon)P^*}{h}+\frac{\sigma_1^2N^*}{2}+\frac{\sigma_2^2P^*}{2}$ *then the system (2) exists a stationary distribution and it is ergodic.*

Proof Let $(N^*,\ P^*)$ be an interior equilibrium point of the system (1) and we define a function $V(N, P)$ as follows:

$$
\begin{aligned}
V(N,\ P) &= N - N^* \ln\left(\frac{N}{N^*}\right) + P - P^* \ln\left(\frac{P}{P^*}\right)\\
LV &= (N - N^*)\frac{N}{N^*} + \frac{\sigma_1^2 N^*}{2} + (P - P^*)\frac{P}{P^*} + \frac{\sigma_2^2 P^*}{2}\\
&= (N - N^*)\left[r\left(1 - \frac{N}{k}\right) - \frac{(\lambda + aP)P}{1 + h(\lambda + aP)N}\right]\\
&+ (P - P^*)\left[\frac{\epsilon(\lambda + aP)N}{1 + h(\lambda + aP)N}\frac{P}{\delta + P} - m - m_1 P\right]\\
&\quad + \frac{\sigma_1^2 N^*}{2} + \frac{\sigma_2^2 P^*}{2}\\
&\le -\frac{r}{k}(N - N^*)^2 - m_1(P - P^*)^2 + \frac{\epsilon(P - P^*)^2}{P^* + \delta} + \frac{(1+\epsilon)(P + P^*)}{h} + \frac{\sigma_1^2 N^*}{2} + \frac{\sigma_2^2 P^*}{2}\\
&= -\frac{r}{k}(N - N^*)^2 - \left(m_1 - \frac{\epsilon}{P^* + \delta}\right)(P - P^*)^2 + \frac{(1+\epsilon)(P + P^*)}{h} + \frac{\sigma_1^2 N^*}{2} + \frac{\sigma_2^2 P^*}{2}\\
&= -\frac{r}{k}(N - N^*)^2 - \left(m_1 - \frac{\epsilon}{P^* + \delta}\right)\left(P - P^* + \frac{(1+\epsilon)(\delta + P^*)}{2h(m_1 P^* - m_1\delta - \epsilon)}\right)^2\\
&\quad + \frac{(1+\epsilon)^2(\delta + P^*)}{4h^2(m_1 P^* - m_1\delta - \epsilon)} + \frac{2(1+\epsilon)P^*}{h} + \frac{\sigma_1^2 N^*}{2} + \frac{\sigma_2^2 P^*}{2}.
\end{aligned}
$$

If $\beta < \min\left\{\left(\frac{r}{k}\right)N^{*2}, \left(m_1 - \frac{\epsilon}{P^* + \delta}\right)\left(P^* - \frac{(1+\epsilon)(\delta + P^*)}{2h(m_1 P^* - m_1\delta - \epsilon)}\right)^2\right\}$, the ellipsoid $\frac{r}{k}(N - N^*)^2 - \left(m_1 + \frac{\epsilon}{P^* + \delta}\right)\left(P - P^* + \frac{(1+\epsilon)(\delta + P^*)}{2h(m_1 P^* - m_1\delta - \epsilon)}\right)^2 = \beta$ lies within $\mathbb{R}^2_+$. We choose U as a neighborhood of the ellipsoid such that $(\bar{U}) \subseteq int(\mathbb{R}^2_+)$, where $(\bar{U})$ is the closure of U. So $LV < 0$ for all $(N,\ P) \in \mathbb{R}^2_+ \backslash U$. Also $A_1 = \min\{\sigma_1^2 N^2, \sigma_2^2 P^2, (N,\ P) \in \bar{U}\} > 0$ such that

$$\sum_{i,\,j=1}^{2} a_{ij}\zeta_i\zeta_j = \sigma_1^2 N^2 \zeta_1^2 + \sigma_2^2 P^2 \zeta_2^2 \ge A_1|\zeta|^2, \text{ for all } (N,\ P) \in \bar{U},\ \zeta \in \mathbb{R}^2.$$

Hence applying the lemma1 we conclude that the system (2) has a stationary distribution $\mu(.)$. □

5.3 Stochastic persistence and extinction

In this subsection, we show that if the initial condition is positive and a certain condition holds then the solution trajectories start from the first quadrant then it always remains in the interior of the first quadrant and the solution remains bounded in future time. Also, there exist some conditions for which the population goes to extinction.

Definition 1 The population $N(t)$ is called strongly persistence in mean if $\lim\limits_{T\to\infty} \inf \frac{1}{T}\int_0^T N(t)dt > 0$.

Lemma 2 *(1) Let μ, T be positive constant and $\lambda \ge 0$ such that $\ln N(t) \le \lambda t - \mu\int_0^t N(s)ds + \sum_{i=1}^{n}\sigma_i B_i(t)$, where σ_i's are constants $(1 \le i \le n)$ for $t \ge T$ then $\lim\limits_{T\to\infty} \sup \frac{1}{T}\int_0^T N(t)dt \le \frac{\lambda}{\mu}$.*

(2) Let μ, T be positive constant and $\lambda \ge 0$ such that $\ln N(t) \ge \lambda t - \mu\int_0^t N(s)ds + \sum_{i=1}^{n}\sigma_i B_i(t)$, where σ_i's are constants $(1 \le i \le n)$ for $t \ge T$ then $\lim\limits_{T\to\infty} \inf \frac{1}{T}\int_0^T N(t)dt \ge \frac{\lambda}{\mu}$.

Theorem 6 *The solution of the stochastic model (2) are strongly persistent in mean if $r > \frac{\sigma_1^2}{2} + (\lambda + a\bar{k})\bar{k}$ and $\left[\frac{\epsilon\lambda k}{rm(1 + h(\lambda + a\bar{k})\bar{k})}\left(r - \frac{\sigma_1^2}{2} - (\lambda + a\bar{k})\bar{k}\right) > \frac{\epsilon}{hm} + 1 + \frac{\sigma_2^2}{2m}\right]$, where $\bar{k}$ is an upper bound of $\{N,\ P\}$.*

Proof Let us define $V_1(N(t)) = \ln(N(t))$. Applying Ito's formula we get

$$dV_1 = \left[r\left(1 - \frac{N(t)}{k}\right) - \frac{(\lambda + aP(t))P(t)}{1 + h(\lambda + aP(t))N(t)} - \frac{\sigma_1^2}{2} \right] dt + \sigma_1 dB_1(t)$$
$$\geq \left(r - \frac{\sigma_1^2}{2} - (\lambda + a\bar{k})\bar{k} \right) dt + \sigma_1 dB_1(t) - \frac{rN}{k} dt.$$

Integrating both sides from the limit 0 to t and we get,

$$\frac{\ln(N(t) - \ln(N(0))}{t} \geq \left(r - \frac{\sigma_1^2}{2} - (\lambda + a\bar{k})\bar{k} \right) + \frac{\sigma_1 B_1(t)}{t} - \frac{r}{kt} \int_0^t N(s) ds.$$

Applying the lemma 2 we say $\lim_{t\to\infty} \inf \frac{1}{t} \int_0^t N(t) dt \geq \frac{k}{r} \left(r - \frac{\sigma_1^2}{2} - (\lambda + a\bar{k})\bar{k} \right) > 0.$

Again we define $V_2(P(t)) = \ln(P(t))$ and using Ito's formula we get,

$$dV_2 = \left[\frac{\epsilon(\lambda + aP)N}{1 + h(\lambda + aP)N} \frac{P}{\delta + P} - m - m_1 P - \frac{\sigma_2^2}{2} \right] dt + \sigma_2 dB_2(t)$$
$$\geq \left[\frac{\epsilon \lambda N}{1 + h(\lambda + a\bar{k})\bar{k}} - \frac{\epsilon}{h} - m - m_1 P - \frac{\sigma_2^2}{2} \right] dt + \sigma_2 dB_2(t).$$

Integrating both sides between the limit 0 to t and using the previous inequality we get,

$$\ln(P(t)) - \ln(P(0)) \geq \left[\frac{\epsilon \lambda k}{r(1 + h(\lambda + a\bar{k})\bar{k})} \left(r - \frac{\sigma_1^2}{2} - (\lambda + a\bar{k})\bar{k} \right) - \frac{\epsilon}{h} - m - \frac{\sigma_2^2}{2} \right] t$$
$$+ \sigma_2 B_2(t) - m_1 \int_0^t P(s) ds.$$

Using the lemma 2 we conclude that $\lim_{t\to\infty} \inf \frac{1}{t} \int_0^t P(t) dt \geq \left[\frac{\epsilon \lambda k}{rm(1 + h(\lambda + a\bar{k})\bar{k})} \left(r - \frac{\sigma_1^2}{2} - (\lambda + a\bar{k})\bar{k} \right) - \frac{\epsilon}{hm} - 1 - \frac{\sigma_2^2}{2m} \right] > 0.$

This complete the proof of the theorem. □

Theorem 7 *If* $\sigma_1^2 > 2r$ *and* $\left(\frac{\epsilon}{h} < m + \frac{\sigma_2^2}{2} \right)$ *then both the population goes to extinction.*

Proof From the above Theorem (6) we see that

$$dV_1 \leq \left(r - \frac{\sigma_1^2}{2} \right) dt + \sigma_1 dB_1(t) - \frac{rN}{k} dt.$$

Integrating both sides and using the lemma (2) we get, $\lim_{t\to\infty} \sup \frac{1}{t} \int_0^t N(t) dt \leq \frac{k}{r} \left(r - \frac{\sigma_1^2}{2} \right) < 0$, which implies $\lim_{t\to\infty} N(t) = 0$. Similarly, we get

$$dV_2 \leq \left(\frac{\epsilon}{h} - m - m_1 P - \frac{\sigma_2^2}{2} \right) dt + \sigma_2 dB_2(t).$$

So integrating and using the lemma (2) we get, $\lim_{t\to\infty} \sup \frac{1}{t} \int_0^t P(t) dt \leq \frac{1}{m_1} \left(\frac{\epsilon}{h} - m - \frac{\sigma_2^2}{2} \right) < 0$, which gives $\lim_{t\to\infty} P(t) = 0$. This completes the proof. □

5.4 Confidence ellipse about interior equilibrium point for stochastic model (2)

In this section, we derive the equation for confidence ellipse about some interior equilibrium point. Let us take the same intensities of environmental fluctuation then the stochastic model (2) can be expressed as

$$dX(t) = a(X)dt + \sigma M(X(t)) dB(t), \tag{15}$$

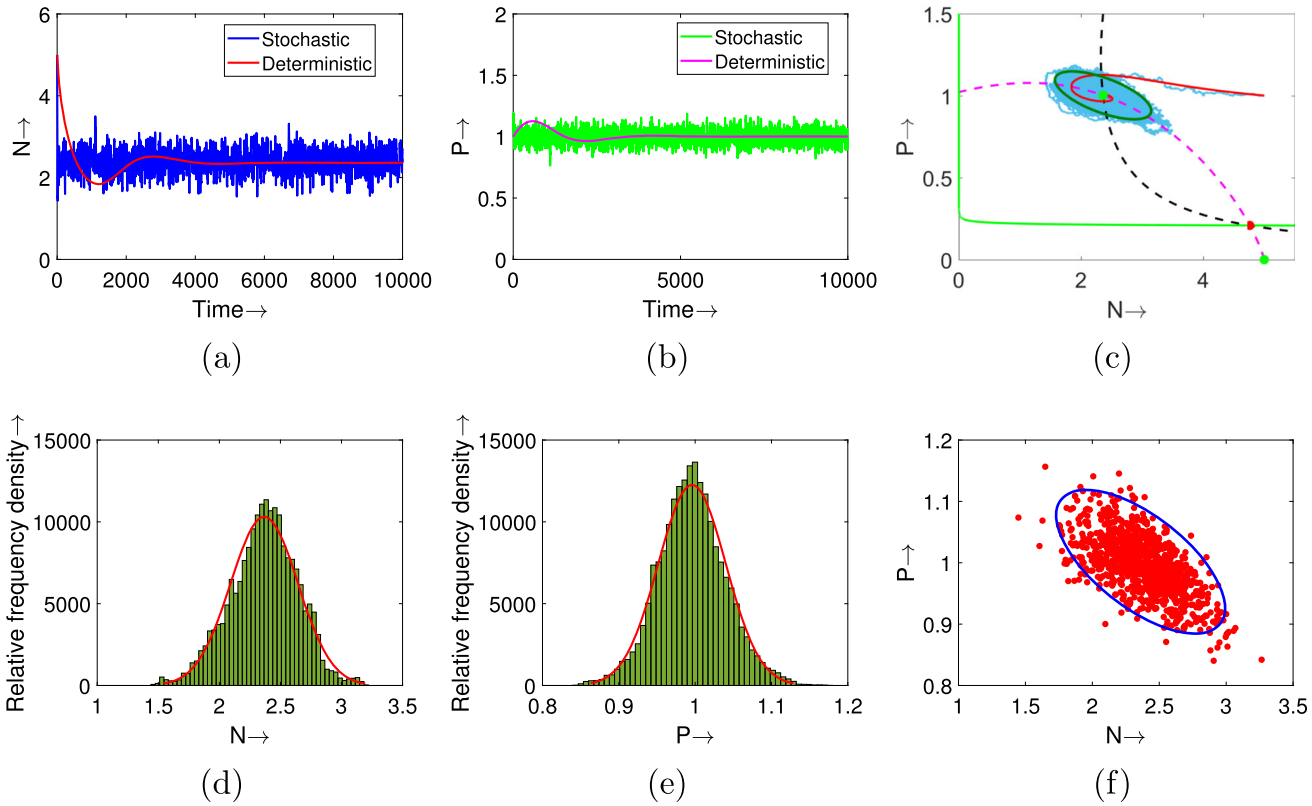

Fig. 12 Time series solutions of systems (1) and (2) and corresponding phase portrait along with confidense ellipse (a-c). Relative frequency density of prey, predator populations and scatter plot along with the confidence ellipse (d-f). We assume $\sigma_1 = \sigma_2 = 0.02$, $k = 5$, $a = 0.6$ and remaing parameters are given in Table 2

where, $a(X) = \begin{pmatrix} rN\left(1 - \frac{N}{k}\right) - \frac{(\lambda + aP)NP}{1 + h(\lambda + aP)N} \\ \frac{\epsilon(\lambda + aP)NP}{1 + h(\lambda + aP)N} \frac{P}{\delta + P} - mP - m_1 P^2 \end{pmatrix}$, $M(X) = \begin{pmatrix} N & 0 \\ 0 & P \end{pmatrix}$.

The quasi-potential function $(V(X))$ is defined by $V(X) = -\lim_{\sigma \to 0} \sigma^2 \ln \Phi(X, \sigma)$ [58]. We consider the approximation of a stable equilibrium solution for the system (15). Let $X^* = (N^*, P^*)$ be the stable equilibrium point and the asymptotic stationary distribution can be represented in the Gaussian form as follows:

$$\Phi(X, \sigma) \approx Ke^{\left(-\frac{V(X)}{\sigma^2}\right)} \approx Ke^{\left(-\frac{(X - X^*)^T W^{-1}(X - X^*)}{2\sigma^2}\right)}. \tag{16}$$

Here $\sigma^2 W$ is the $n \times n$ covariance matrix. The stationary distribution function $\Phi(x, \sigma)$ control the oscillation of the solution of the system (15). The element of the matrix W satisfies the following equations [59, 60]:

$$GW + WG^T = -A(X),\ G = \frac{\partial F}{\partial X}(X^*),$$

where, A is the diffusion matrix. If we assume that $W = \begin{pmatrix} w_{11} & w_{12} \\ w_{21} & w_{22} \end{pmatrix}$ and $G = \begin{pmatrix} h_{11} & h_{12} \\ h_{21} & h_{22} \end{pmatrix}$ then we get the following equations:

$$\begin{aligned} 2h_{11}w_{11} + h_{12}w_{12} + h_{12}w_{21} + {N_*}^2 &= 0, \\ h_{21}w_{11} + (h_{11} + h_{22})w_{12} + h_{12}w_{22} &= 0, \\ h_{21}w_{11} + (h_{11} + h_{22})w_{21} + h_{12}w_{22} &= 0, \\ h_{21}w_{12} + h_{21}w_{21} + 2h_{22}w_{22} + {P_*}^2 &= 0. \end{aligned}$$

Solving the above equation, we get the stochastic sensitivity matrix W. Therefore the equation of confidence ellipse can be written as

$$(X - X^*)^T W^{-1}(X - X^*) = -2\sigma^2 \ln(1 - p), \tag{17}$$

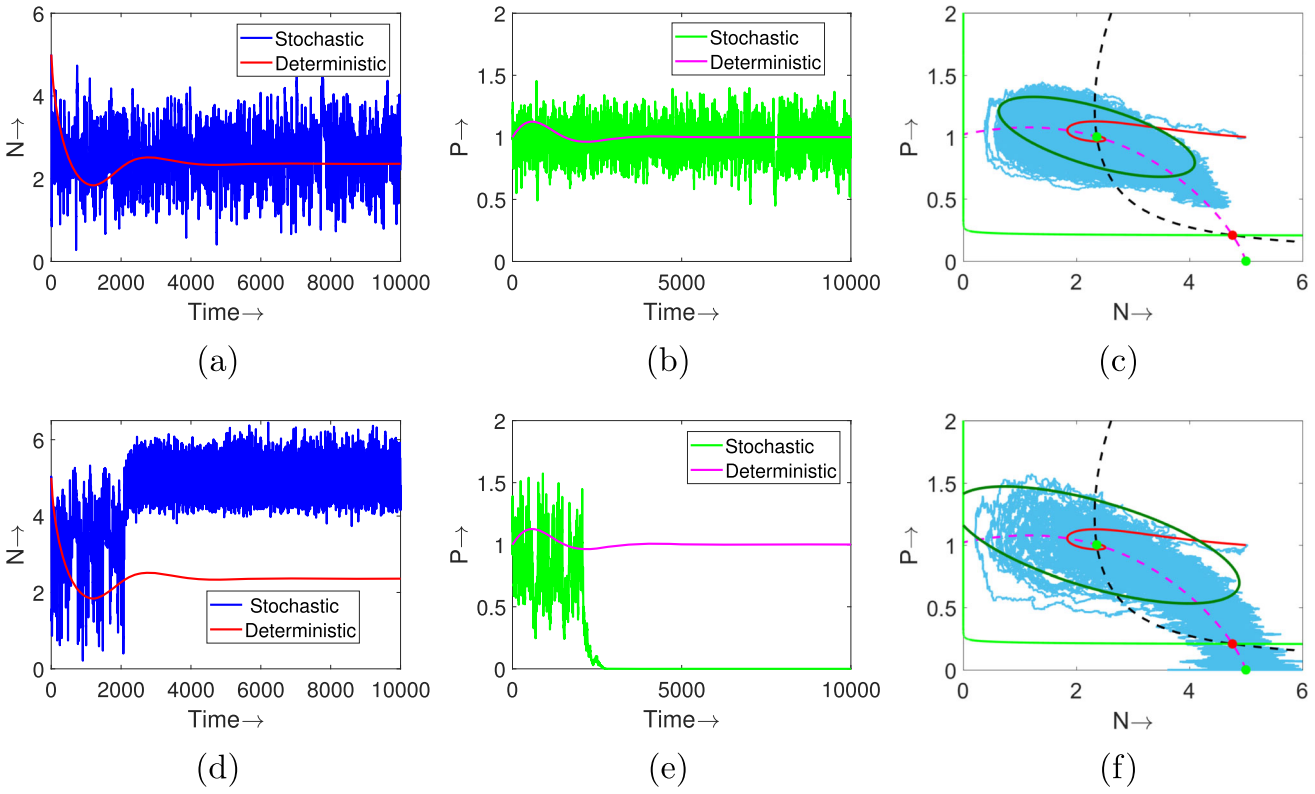

Fig. 13 We assume $k = 5$ and $a = 0.6$ and other parameters are given in Table-2. For the intensities of environmental fluctuation $\sigma_1 = 0.05$, $\sigma_2 = 0.05$ the deterministic vs stochastic solution of (2) for Prey and Predator shown in $(a - b)$ and corresponding phase portrait with confidence ellipse (cyan) is shown in (c). Regime shift for prey (d) and predator (e) for the intensities $\sigma_1 = 0.1$, $\sigma_2 = 0.1$ and all the parameters are same as before. Corresponding phase portrait with confidence ellipse is shown in (f)

where p is called fiducial probability.

6 Numerical simulation for stochastic model

Here, we shall verify the theoretical result for a stochastic model with the help of numerical simulation. We use Milstein's higher-order approximation method [61] then we obtain the following discretization system:

$$N_{i+1} = N_i + \left[rN_i\left(1 - \frac{N_i}{k}\right) - \frac{(\lambda + aP_i)N_iP_i}{1 + h(\lambda + aP_i)N_i}\right]\Delta t + \sigma_1 N_i a_i\sqrt{\Delta t} + \frac{\sigma_1^2}{2}N_i(a_i^2 - 1)\Delta t$$

$$P_{i+1} = P_i + \left[\frac{\epsilon(\lambda + aP_i)N_iP_i}{1 + h(\lambda + aP_i)N_i}\frac{P_i}{\delta + P_i} - mP_i - m_1{P_i}^2\right]\Delta t + \sigma_2 P_i b_i\sqrt{\Delta t} + \frac{\sigma_2^2}{2}P_i(b_i^2 - 1)\Delta t.$$

Where $\Delta t > 0$ and a_i, b_i are the independent Gaussian random variables $N(0, 1)$ for $i = 1, 2, 3, ..., n$.

To start numerical simulation for the stochastic model (2), we consider the parametric values given in Table 2 except $a = 0.6$ and $k = 5$. In this case, we see that there exists two interior equilibrium points where higher density equilibrium point is stable spiral and another equilibrium point is saddle. From Figs. 12 (a) and 12 (b), we see that the deterministic solution is stable for both prey and predator population. If we increase the environmental white noises $\sigma_1 = 0.02$ and $\sigma_2 = 0.02$ then the solution of the system (2) fluctuate around the deterministic steady state values $N^* = 2.36089$, $P^* = 1.00164$. We have repeated the simulation 10000 times and taken all parameters fixed and observe no extinction scenario. It can be verified that no extinction will for the future time for the chosen parameters and intensities. The corresponding phase portrait for both populations is shown in Fig. 12(c). Also, the stationary distribution for both populations is shown in Fig. 12(d) and 12(e). From the stationary distribution, it is clear that the population distributed normally about the mean values $N^* = 2.36089$ and $P^* = 1.00164$ respectively. The spread of the stationary distribution is influenced by the strength of environmental fluctuations. A stochastic stable system can be visualized as a probability cloud representing the stationary distribution. In Fig. 12(f), we depict a scatter diagram for both populations, illustrating how the probability cloud fluctuates around the deterministic stable equilibrium point (2.36089, 1.00164). The dispersion of this cloud is

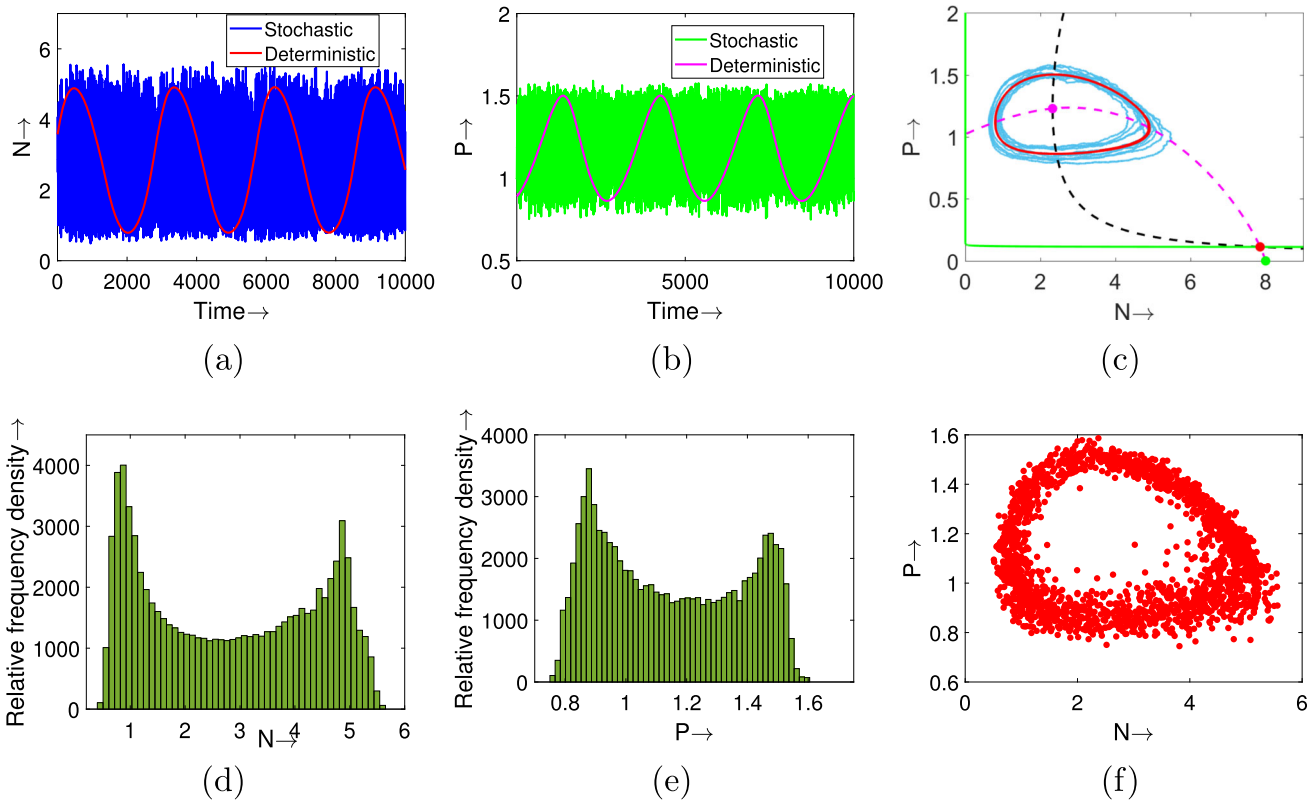

Fig. 14 Time series for deterministic vs stochastic solution for prey and predator $(a - b)$ and the corresponding phase portrait shown in (c). The stationary distribution for prey and predator is shown in d and e. The scatter plot is shown in f. We assume $\sigma_1 = 0.01$, $\sigma_2 = 0.01$, $k = 8$ and $a = 0.6$. and other parameters are given in Table 2

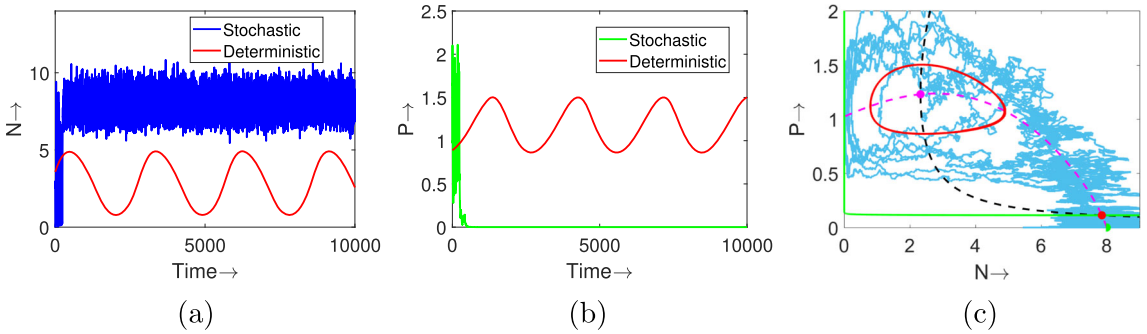

Fig. 15 Time series for prey and predator in deterministic and stochastic solution $(a - b)$ for $\sigma_1 = 0.1$, $\sigma_2 = 0.1$, $a = 0.6$, $k = 8$ and other parameters are given in Table 2. The corresponding phase portrait is shown in (c)

determined by the intensities σ_1 and σ_2, reflecting the magnitude of environmental fluctuations affecting the prey and predator populations.

Also, we plot the confidence ellipse about the interior equilibrium point $E_1^*(2.36080,\ 1.00164)$ using the following equation for $\sigma_1 = \sigma_2 = \sigma = 0.02$ and fiducial probability $p = 0.95$

$$0.01034(x - 2.36080)^2 + 0.07197(x - 2.36080)(y - 1.00164) + 0.29984(y - 1.00164)^2 + 2\sigma^2 \ln(1 - p) = 0 \text{ (see Fig. 12(c))}. \tag{18}$$

If we increase the strength of fluctuation as $\sigma_1 = \sigma_2 = 0.05$ then the oscillation is highly fluctuate (Figs. 13(a-b)). Also, the interesting fact is that the size of confidence ellipse increase from earlier (Fig. 13(c)). The stochastic solution started to shift from one region to another when we increase the strength of fluctuation as $\sigma_1 = \sigma_2 = 0.1$. We see that the confidence ellipse crosses the basin of attraction and so the prey population shifted from its stable point 2.36089 to 4.761985175 and similar way the predator population shifted from stable equilibrium point 1.00164 to extinction (Figs 13(d-e)). The corresponding phase portrait is shown in (Fig. 13(f)) and this is known as regime shift in the stochastic model (2).

In the next step, we consider the parametric values from Table 2 except $k = 8$ and $a = 0.6$. Then we see from Figs. 14$(a - b)$ that the solution of the deterministic model is unstable with stable limit cycle. If we introduce environmental white noise $\sigma_1 = 0.01$, $\sigma_2 = 0.01$ then we see that the periodic solution is oscillate about its deterministic solution. The corresponding phase portrait is shown in Figs. 14(c) and from this we see that due to environmental fluctuation the solution oscillates around the stable limit cycle. The stationary distribution is shown in Figs. 14$(d - e)$ and it is clear that the prey population is distributed within (0.1, 5.9) and the range for the predator population is (0, 6). In Fig. 14(f) we see the probability cloud of stationary distribution up to $t = 1000$. It is clear that the probability cloud is distributed about the limit cycle and it remains unchanged at future times.

If we increase the strength of fluctuation then the system changes its dynamic behaviour. To verify this we increase the strength of white noise $\sigma_1 = \sigma_2 = 0.1$ and take all other parameters fixed then we see from Figs. 15$(a - b)$ that the prey population shifted from one region to other but never goes to extinction whereas the predator population goes to extinction.

7 Conclusion

In this paper, we have analyzed a prey-predator model with hunting cooperation and mate-finding Allee effect in both deterministic and stochastic environments. The purpose of this study is to investigate hunting cooperation in the presence of the Allee effect. Here, we have examined the equilibria and their local stability. Furthermore, we have determined that the deterministic system experiences saddle-node and Hopf-bifurcations. By increasing the prey growth rate, carrying capacity, and attack rate of a predator, the system becomes unstable from its stable nature. However, the Allee effect can stabilize the system. Moreover, we found that the system exhibits complex dynamics with an increase in carrying capacity, predator attack rates, hunting cooperation, and Allee effect values for another set of values.

Due to the importance of white noise to the population dynamics of ecological systems, we also investigated the behavior of a stochastic system that corresponds to our proposed model. A global positive solution to the stochastic system can be determined analytically under certain conditions. For low intensities of environmental noise, the solution trajectories of our stochastic system fluctuate near those of the corresponding deterministic system. The amplitudes of fluctuations increase with gradual increases in white noise intensities. We observed due to high fluctuations the regime shift occur and we use SSF technique to show the shifting behavior. Depending on different intensities of environmental fluctuation the size of the confidence ellipse changes and the dynamical behavior changes when it crosses the separatrix. Overall, we observed that the fluctuations in the equilibrium abundances of prey and predator species in the ecosystem can be minimized by regulating the intensities of the environmental noises. According to stochastic simulation results, at lower noise strength levels, population density will be subject to random fluctuations. It is important to note that our stochastic system is prone to noise-induced transitions.

In this paper, we have examined both the deterministic and stochastic effects of our system. In our future direction, we aim to incorporate delay into our model and explore its implications. Additionally, we plan to study the system within an imprecise environment by introducing interval numbers. By integrating delay and imprecision into our analysis, we anticipate gaining a deeper understanding of the dynamics of ecological systems and their responses to various factors. This extension will enable us to investigate how delayed interactions and parameter uncertainties influence system behavior, offering valuable insights into ecological processes and ecosystem stability.

Author Contributions **Biswajit Paul:** Formal analysis, Writing - original draft, Simulations. **Bapin Mondal:** Formal analysis, Writing - review and editing, Simulations, Conceptualization. **Uttam Ghosh** Conceptualization, Supervision.

Funding Not applicable.

Declarations

Conflict of interest The authors declare that there is no conflict of interest in publishing this paper.

Appendices

Appendix A

$$A = ka^2h^2m_1^2,\ B = 2kahm_1(a\delta hm_1 + ahm + h\lambda m_1 - a\epsilon),$$
$$C = k(a^2\delta^2h^2m_1^2 + 4a^2\delta h^2mm_1 + 4a\delta h^2\lambda m_1^2 - 2a^2\delta\epsilon hm_1 + a^2h^2m^2 + 4ah^2\lambda mm_1 + h^2\lambda^2m_1^2 - 2a^2\epsilon hm - 4a\epsilon h\lambda m_1 + a^2\epsilon^2),$$
$$D = k(2a^2\delta^2h^2mm_1 + 2a\delta^2h^2\lambda m_1^2 + 2a^2\delta h^2m^2 + 8a\delta h^2\lambda mm_1 + 2\delta h^2\lambda^2m_1^2 - 2a^2\delta\epsilon hm - 4a\delta\epsilon h\lambda m_1 + 2ah^2\lambda m^2 + 2h^2\lambda^2mm_1$$
$$- 4a\epsilon h\lambda m + a\epsilon hm_1r - 2\epsilon h\lambda^2m_1 + 2a\epsilon^2\lambda),$$
$$E = ka^2\delta^2h^2m^2 + 4ka\delta^2h^2\lambda mm_1 + k\delta^2h^2\lambda^2m_1^2 + 4ka\delta h^2\lambda m^2 + 4k\delta h^2\lambda^2mm_1 - 4ka\delta\epsilon h\lambda m + ka\delta\epsilon hm_1r - 2k\delta\epsilon h\lambda^2m_1 + kh^2\lambda^2m^2$$

$+ ka\epsilon hmr - 2k\epsilon h\lambda^2 m + k\epsilon h\lambda m_1 r - ka\epsilon^2 r + k\epsilon^2\lambda^2 + \epsilon m_1 r,$

$F = 2ka\delta^2 h^2\lambda m^2 + 2k\delta^2 h^2\lambda^2 m m_1 + 2k\delta h^2\lambda^2 m^2 + ka\delta\epsilon hmr - 2k\delta\epsilon h\lambda^2 m + k\delta\epsilon h\lambda m_1 r + k\epsilon h\lambda mr$

$- k\epsilon^2\lambda r + \delta\epsilon m_1 r + \epsilon mr,\ G = \delta m(k\delta h^2\lambda^2 m + k\epsilon h\lambda r + \epsilon r).$

Appendix B

$$a_{11} = \frac{N^* hr^2}{P^*}\left(1 - \frac{N^*}{k}\right)^2 - \frac{rN^*}{k},\ a_{12} = -\frac{N^*(\lambda + 2P^* a + N^* h(\lambda + aP^*)^2)}{(1 + N^* h(\lambda + aP^*))^2},$$
$$a_{21} = \frac{P^*(m + m_1 P^*)}{N^*},\ a_{22} = m - \frac{(m + m_1 P^*)^2(\lambda + N^* h(\lambda + aP^*)^2 - aP^*)}{\epsilon N^*(\lambda + aP^*)^2}.$$

Appendix C

$$f_{NN} = -\frac{2r}{k} + \frac{2P^* h(\lambda + aP^*)^2}{(1 + N^* h(\lambda + aP^*))^3},\ f_{NP} = -\frac{N^* h\lambda(\lambda + aP^* + \lambda + 2aP^*)}{(1 + N^* h(\lambda + aP^*))^3},\ f_{PP} = -\frac{2aN^*(1 + \lambda h N^*)}{(1 + N^* h(\lambda + aP^*))^3},$$
$$g_{NN} = -\frac{2\epsilon P^{*2} h(\lambda + aP^*)^2}{(1 + N^* h(\lambda + aP^*))^3(\delta + P^*)},$$
$$g_{NP} = \frac{\epsilon p^*(N^* P^{*2} a^2\delta h + N^* P^{*2} a\lambda h + 3N^* P^* a\delta h + N^* P^*\lambda^2 h + 2N^*\delta h\lambda^2 + 2P^{*2} a + 3P^* a\delta + P^*\lambda + 2\delta\lambda)}{(1 + N^* h(\lambda + aP^*))^3(\delta + P^*)^2},$$
$$g_{PP} = \frac{1}{(1 + N^* h(\lambda + aP^*))^3(\delta + P^*)^2}(2\epsilon N^*(N^{*2}\delta^2 h^2(\lambda + aP^*)^3 + N^* P^{*3} a^2\delta h + 3N^* P^{*2} a^2\delta^2 h + N^* P^{*3} a\lambda h + 3N^* P^{*2} a\delta\lambda h$$
$$+ 6N^* P^* a\delta^2 h\lambda + 2N^*\delta^2 h\lambda^2 + a(\delta + P^*)^3 + \delta^2\lambda - \delta^3 a)).$$

Appendix D

$$k_{20} = \alpha_{20} + \frac{a(r) - \alpha_{10}}{\alpha_{01}}\alpha_{11} + \left(\frac{a(r) - \alpha_{10}}{\alpha_{01}}\right)^2\alpha_{02},$$
$$k_{11} = \frac{b(r)}{\alpha_{01}}\alpha_{11} + 2\left(\frac{a(r) - \alpha_{10}}{\alpha_{01}}\right)\frac{b(r)}{\alpha_{01}}\alpha_{02},$$
$$k_{02} = \left(\frac{b(r)}{\alpha_{01}}\right)^2\alpha_{02},$$
$$k_{30} = \left(\frac{\alpha(r) - \alpha_{10}}{\alpha_{01}}\right)^2\alpha_{12} + \left(\frac{a(r) - \alpha_{10}}{\alpha_{01}}\right)^3\alpha_{03},$$
$$k_{21} = 2\left(\frac{a(r) - \alpha_{10}}{\alpha_{01}}\right)\frac{b(r)}{\alpha_{01}}\alpha_{12} + 3\left(\frac{a(r) - \alpha_{10}}{\alpha_{01}}\right)^2\frac{b(r)}{\alpha_{01}}\alpha_{03},$$
$$k_{12} = 3\left(\frac{a(r) - \alpha_{10}}{\alpha_{01}}\right)\left(\frac{b(r)}{\alpha_{01}}\right)^2\alpha_{03} + \left(\frac{b(r)}{\alpha_{01}}\right)^2\alpha_{12},$$
$$k_{03} = \left(\frac{b(r)}{\alpha_{01}}\right)^3\alpha_{03},$$
$$l_{20} = \frac{\alpha_{01}}{b(r)}\left\{\left(\frac{a(r) - \alpha_{10}}{\alpha_{01}}\right)^2\beta_{02} + \frac{a(r) - \alpha_{10}}{\alpha_{01}}\beta_{11} - \left(\alpha_{20} + \frac{a(r) - \alpha_{10}}{\alpha_{01}}\alpha_{11} + \left(\frac{a(r) - \alpha_{10}}{\alpha_{01}}\right)^2\alpha_{02}\right)\frac{a(r) - \alpha_{10}}{\alpha_{01}}\right\},$$
$$l_{11} = \frac{\alpha_{01}}{b(r)}\left\{\frac{b(r)}{\alpha_{01}}\beta_{11} + 2\left(\frac{a(r) - \alpha_{10}}{\alpha_{01}}\right)\frac{b(r)}{\alpha_{01}}\beta_{02} - \frac{a(r) - \alpha_{10}}{\alpha_{01}}\left(\frac{b(r)}{\alpha_{01}}\alpha_{11} + 2\left(\frac{a(r) - \alpha_{10}}{\alpha_{01}}\right)\frac{b(r)}{\alpha_{01}}\alpha_{02}\right)\right\},$$
$$l_{02} = \frac{\alpha_{01}}{b(r)}\left\{\left(\frac{b(r)}{\alpha_{01}}\right)^2\beta_{02} - \frac{a(r) - \alpha_{10}}{\alpha_{01}}\frac{b(r)}{\alpha_{01}}\alpha_{02}\right\},\ l_{03} = \frac{\alpha_{01}}{b(r)}\left\{\left(\frac{b(r)}{\alpha_{01}}\right)^3\beta_{03} - \frac{a(r) - \alpha_{10}}{\alpha_{01}}\left(\frac{b(r)}{\alpha_{01}}\right)^3\alpha_{03}\right\},$$
$$l_{30} = \frac{\alpha_{01}}{b(r)}\left\{\left(\frac{a(r) - \alpha_{10}}{\alpha_{01}}\right)^2\beta_{12} + \left(\frac{a(r) - \alpha_{10}}{\alpha_{01}}\right)^3\beta_{03} - \left(\left(\frac{a(r) - \alpha_{10}}{\alpha_{01}}\right)^2\alpha_{12} + \left(\frac{a(r) - \alpha_{10}}{\alpha_{01}}\right)^3\alpha_{03}\right)\frac{a(r) - \alpha_{10}}{\alpha_{01}}\right\},$$
$$l_{21} = \frac{\alpha_{01}}{b(r)}\left\{2\left(\frac{a(r) - \alpha_{10}}{\alpha_{01}}\right)\frac{b(r)}{\alpha_{01}}\beta_{12} + 3\left(\frac{a(r) - \alpha_{10}}{\alpha_{01}}\right)^2\frac{b(r)}{\alpha_{01}}\beta_{03} - \left(2\left(\frac{a(r) - \alpha_{10}}{\alpha_{01}}\right)\frac{b(r)}{\alpha_{01}}\alpha_{12}\right.$$
$$\left. + 3\left(\frac{a(r) - \alpha_{10}}{\alpha_{01}}\right)^2\frac{b(r)}{\alpha_{01}}\alpha_{03}\right)\frac{a(r) - \alpha_{10}}{\alpha_{01}}\right\},$$

$$l_{12} = \frac{\alpha_{01}}{b(r)}\left\{3\left(\frac{a(r)-\alpha_{10}}{\alpha_{01}}\right)\left(\frac{b(r)}{\alpha_{01}}\right)^2\beta_{03} + \left(\frac{b(r)}{\alpha_{01}}\right)^2\beta_{12} - \left(3\left(\frac{a(r)-\alpha_{10}}{\alpha_{01}}\right)\left(\frac{b(r)}{\alpha_{01}}\right)^2\alpha_{03} + \left(\frac{b(r)}{\alpha_{01}}\right)^2\alpha_{12}\right)\frac{a(r)-\alpha_{10}}{\alpha_{01}}\right\}$$

References

1. H. I. Freedman, Deterministic mathematical models in population ecology, Vol. 57, Marcel Dekker Incorporated, (1980)
2. A. J. Lotka, A natural population norm. i, Journal of the Washington Academy of Sciences 3 (9) 241–248 (1913)
3. D. Sen, S. Ghorai, M. Banerjee, Allee effect in prey versus hunting cooperation on predator-enhancement of stable coexistence. International Journal of Bifurcation and Chaos **29**(06), 1950081 (2019)
4. V. Volterra, Fluctuations in the abundance of a species considered mathematically. Nature **118**(2972), 558–560 (1926)
5. S. Pimm, J.H. Lawton, On feeding on more than one trophic level. Nature **275**(5680), 542–544 (1978)
6. R. M. May, Stability and complexity in model ecosystems, Princeton university press, (2019)
7. S.G. Mortoja, P. Panja, S.K. Mondal, Dynamics of a predator-prey model with nonlinear incidence rate, crowley-martin type functional response and disease in prey population. Ecological Genetics and Genomics **10**, 100035 (2019)
8. K. Watt, A mathematical model for the effect of densities of attacked and attacking species on the number attacked. The Canadian Entomologist **91**(3), 129–144 (1959)
9. M. Hassell, J. Lawton, J. Beddington, The components of arthropod predation: I. the prey death-rate, The Journal of Animal Ecology 135–164 (1976)
10. S.G. Mortoja, P. Panja, S.K. Mondal, Dynamics of a predator-prey model with stage-structure on both species and anti-predator behavior. Informatics in medicine unlocked **10**, 50–57 (2018)
11. R. Kneib, Testing for indirect effects of predation in an intertidal soft-bottom community. Ecology **69**(6), 1795–1805 (1988)
12. L. Berec, Impacts of foraging facilitation among predators on predator-prey dynamics. Bulletin of mathematical biology **72**, 94–121 (2010)
13. S. Creel, N.M. Creel, Communal hunting and pack size in african wild dogs, lycaon pictus. Animal Behaviour **50**(5), 1325–1339 (1995)
14. I. Bailey, J.P. Myatt, A. Wilson, Group hunting within the carnivora: physiological, cognitive and environmental influences on strategy and cooperation. Behavioral ecology and sociobiology **67**, 1–17 (2013)
15. C. Feh, T. Boldsukh, C. Tourenq, Are family groups in equids a response to cooperative hunting by predators? the case of mongolian kulans (equus hemionus luteus matschie). Revue d'Ecologie, Terre et Vie **49**(1), 11–20 (1994)
16. M.T. Alves, F.M. Hilker, Hunting cooperation and allee effects in predators. Journal of theoretical biology **419**, 13–22 (2017)
17. S. Pal, N. Pal, J. Chattopadhyay, Hunting cooperation in a discrete-time predator-prey system. International Journal of Bifurcation and Chaos **28**(07), 1850083 (2018)
18. B. Paul, B. Mondal, J.K. Ghosh, U. Ghosh, Dynamic interactions between prey and predator with cooperation and allee effect: Deterministic and stochastic approach. Journal of Biological Systems **30**(04), 799–836 (2022)
19. K. Ryu, W. Ko, Asymptotic behavior of positive solutions to a predator-prey elliptic system with strong hunting cooperation in predators. Physica A: Statistical Mechanics and Its Applications **531**, 121726 (2019)
20. S. Pal, N. Pal, S. Samanta, J. Chattopadhyay, Effect of hunting cooperation and fear in a predator-prey model. Ecological Complexity **39**, 100770 (2019)
21. S. Pal, N. Pal, S. Samanta, J. Chattopadhyay, Fear effect in prey and hunting cooperation among predators in a leslie-gower model. Mathematical Biosciences and Engineering **16**(5), 5146 (2019)
22. A.M. Kramer, B. Dennis, A.M. Liebhold, J.M. Drake, The evidence for allee effects. Population Ecology **51**, 341–354 (2009)
23. B. Dennis, Allee effects: population growth, critical density, and the chance of extinction. Natural Resource Modeling **3**(4), 481–538 (1989)
24. W. Allee, Animal aggregations: A study in general sociology. chicago: Chicago univ. press
25. P.A. Stephens, W.J. Sutherland, Consequences of the allee effect for behaviour, ecology and conservation. Trends in ecology & evolution **14**(10), 401–405 (1999)
26. D.S. Boukal, M.W. Sabelis, L. Berec, How predator functional responses and allee effects in prey affect the paradox of enrichment and population collapses. Theoretical Population Biology **72**(1), 136–147 (2007)
27. F.M. Hilker, Population collapse to extinction: the catastrophic combination of parasitism and allee effect. Journal of Biological Dynamics **4**(1), 86–101 (2010)
28. A. Morozov, S. Petrovskii, B.-L. Li, Spatiotemporal complexity of patchy invasion in a predator-prey system with the allee effect., Journal of theoretical Biology 238 (1) 18–35 (2006)
29. L. Berec, E. Angulo, F. Courchamp, Multiple allee effects and population management. Trends in Ecology & Evolution **22**(4), 185–191 (2007)
30. F. Courchamp, L. Berec, J. Gascoigne, Allee effects in ecology and conservation, OUP Oxford, (2008)
31. B. Dennis, Allee effects in stochastic populations. Oikos **96**(3), 389–401 (2002)
32. M.B. Bonsall, A. Hastings, Demographic and environmental stochasticity in predator-prey metapopulation dynamics. Journal of Animal Ecology **73**(6), 1043–1055 (2004)
33. A. Hening, D. H. Nguyen, Coexistence and extinction for stochastic kolmogorov systems
34. M. Benaïm, S.J. Schreiber, Persistence and extinction for stochastic ecological models with internal and external variables. Journal of mathematical biology **79**, 393–431 (2019)
35. A. Gökçe, Dynamical behaviour of a predator-prey system encapsulating the fear affecting death rate of prey and intra-specific competition: Revisited in a fluctuating environment. Journal of Computational and Applied Mathematics **421**, 114849 (2023)
36. G. Lan, Y. Fu, C. Wei, S. Zhang, Dynamical analysis of a ratio-dependent predator-prey model with holling iii type functional response and nonlinear harvesting in a random environment. Advances in Difference Equations **2018**, 1–25 (2018)
37. M. Liu, K. Wang, Survival analysis of stochastic single-species population models in polluted environments. Ecological Modelling **220**(9–10), 1347–1357 (2009)
38. S. Zhang, S. Yuan, T. Zhang, A predator-prey model with different response functions to juvenile and adult prey in deterministic and stochastic environments. Applied Mathematics and Computation **413**, 126598 (2022)
39. M. Bandyopadhyay, J. Chattopadhyay, Ratio-dependent predator-prey model: effect of environmental fluctuation and stability. Nonlinearity **18**(2), 913 (2005)
40. M. Liu, K. Wang, Q. Wu, Survival analysis of stochastic competitive models in a polluted environment and stochastic competitive exclusion principle. Bulletin of mathematical biology **73**, 1969–2012 (2011)
41. B. Mondal, A. Sarkar, N. Sk, S.S. Santra, T. Muhammad, Exploring resilience, chaos, and bifurcations in a discrete food web model incorporating the mate finding allee effect. The European Physical Journal Plus **138**(11), 1018 (2023)

42. R.H. Kraichnan, Dynamics of nonlinear stochastic systems. Journal of Mathematical Physics **2**(1), 124–148 (1961)
43. Y.-L. Liu, L.-Y. Hao, Adaptive tracking differentiator control for nonlinear stochastic systems, in, 13th Asian Control Conference (ASCC). IEEE **2022**, 512–517 (2022)
44. S. Han, S.-J. Chung, Incremental nonlinear stability analysis of stochastic systems perturbed by lévy noise. International Journal of Robust and Nonlinear Control **32**(12), 7174–7201 (2022)
45. Z. Hu, X. Mu, Event-triggered impulsive control for nonlinear stochastic systems. IEEE Transactions on Cybernetics **52**(8), 7805–7813 (2021)
46. B. Mondal, S. Sarkar, U. Ghosh, Complex dynamics of a generalist predator-prey model with hunting cooperation in predator. The European Physical Journal Plus **137**(1), 43 (2021)
47. J. Sotomayor, Generic bifurcations of dynamical systems, in: Dynamical systems, Elsevier, pp. 561–582 (1973)
48. J. E. Marsden, M. McCracken, The Hopf bifurcation and its applications, Vol. 19, Springer Science & Business Media, (2012)
49. A. H. Nayfeh, B. Balachandran, Applied nonlinear dynamics: analytical, computational, and experimental methods, John Wiley & Sons, (2008)
50. M. Han, P. Yu, Normal forms, Melnikov functions and bifurcations of limit cycles, Vol. 181, Springer, (2012)
51. J. Guckenheimer, Dynamical systems, and bifurcatins of vector fields, Appl. Math. Sci. Series 42
52. S. Wiggins, S. Wiggins, M. Golubitsky, Introduction to applied nonlinear dynamical systems and chaos, Vol. 2, Springer, (2003)
53. B. Mondal, K. Senapati, S. Pandey, U. Ghosh, Consequences of allee effect on the multiple limit cycles in a predator-prey model. The European Physical Journal Plus **138**(10), 919 (2023)
54. A. Friedman, Stochastic differential equations and applications, Courier Corporation, (2012)
55. X. Mao, Stochastic differential equations and applications, Elsevier, (2007)
56. V. Goodman, L. arnold, stochastic differential equations: theory and applications, and av balakrishnan, stochastic differential systems. i: Filtering and control, a function space approach
57. E. Allen, Modeling with Itô stochastic differential equations, Vol. 22, Springer Science & Business Media, (2007)
58. I. Bashkirtseva, L. Ryashko, Constructive analysis of noise-induced transitions for coexisting periodic attractors of the lorenz model. Physical Review E **79**(4), 041106 (2009)
59. L. Ryashko, I. Bashkirtseva, Stochastic sensitivity analysis and control for ecological model with the allee effect. Mathematical Modelling of Natural Phenomena **10**(2), 130–140 (2015)
60. N. Sk, B. Mondal, A.A. Thirthar, M.A. Alqudah, T. Abdeljawad, Bistability and tristability in a deterministic prey-predator model: Transitions and emergent patterns in its stochastic counterpart. Chaos, Solitons & Fractals **176**, 114073 (2023)
61. D.J. Higham, An algorithmic introduction to numerical simulation of stochastic differential equations. SIAM review **43**(3), 525–546 (2001)